Power requirements of biogas upgrading by water scrubbing and biomethane compression: comparative analysis of various plant configurations

Wojciech M. Budzianowski[a,b,*], Christophe E. Wylock[c], Przemysław A. Marciniak[b]

[a] Wrocław University of Technology, Wybrzeże Wyspiańskiego 27, 50-370 Wrocław, Poland

[b] Renewable Energy and Sustainable Development (RESD) Group, Poleska 11/37, 51-354 Wrocław, Poland

[c] Université Libre de Bruxelles, Transfers, Interfaces and Processes (TIPs), Av. F. Roosevelt 50, CP 165/67 - 1050 Brussels, Belgium

[*] Corresponding author. Email address: wojciech.budzianowski@gmail.com

Abstract

Biogas upgrading by water scrubbing followed by biomethane compression is an environmentally benign process. It may be achieved using various plant configurations characterised by various power requirements with associated effects on biomethane sustainability. Therefore, the current study has been undertaken to systematically investigate the power requirements of a range of water scrubbing options. Two groups of water scrubbing are analysed: (1) high pressure water scrubbing (HPWS) and (2) near-atmospheric pressure water scrubbing (NAPWS). A water scrubbing plant model is constructed, experimentally validated and simulated for seven upgrading plant configurations. Simulation results show that the power requirement of biogas upgrading in HPWS plants is mainly associated with biogas compression while in NAPWS plants a significant power is required for water pumping. Biomethane compression to 20 MPa also contributes remarkably. It isobserved that the lowest specific power requirement can be obtained for a NAPWS plant without water regeneration (0.24 kWh/Nm^3 raw biogas) but this plant requires cheap water supply, e.g. outlet water from a sewage treatment plant or river. The second is HPWS without flash (0.29 kWh/Nm^3 raw biogas). All other HPWS with flash and NAPWS with water regeneration plants have specific power requirements between 0.30 and 0.33 kWh/Nm^3 raw biogas. Biogas compression without upgrading requires about 0.29 kWh/Nm^3 raw biogas. The thermodynamic efficiency of biogas upgrading is between 2.2 and 9.8% depending on the plant configuration while biomethane compression efficiency is higher, about 55%. This result implies that the upgrading process has a remarkable potential for improvement whereas compression is very close to its thermodynamic limit. The potential for minimising energy dissipation in the state-of-the-art HPWS upgrading plant with flash by applying a rotary hydraulic pumping device is evaluated at about 0.036 kWh/Nm^3 raw biogas meaning the specific power requirement reduction of 10%.

Keywords

Biogas; biomethane; water scrubbing; plant configuration; power requirements; thermodynamic efficiency; rotary hydraulic pumping device

1. Introduction

Biogas is a renewable and sustainable fuel derived from digestible biomass that is suitable for natural gas substitution. However, biogas generated through anaerobic digestion is of low pressure, low specific gravity and large specific volume. The large share of CO_2 present in biogas lowers its calorific value, flame velocity and flammability limits compared to natural gas. Besides, the transportation of biomethane over longer distances is less costly than the transportation of CO_2 diluted biogas. These challenges may adversely affect biogas sustainability. Therefore, biogas upgrading to biomethane with subsequent use as a natural gas substitute attracts significant attention.

Biomethane, used directly as automotive fuel or being injected into the natural gas grid, has been identified as an important renewable fuel in Europe [1]. Current biomethanation technologies consume less than about 20% of biogas energy for upgrading and compression purposes. Thus biomethanation enables transforming more than about 80% of the energy content of raw biogas into the usable form of clean energy. In addition, biomethanation generates little or no low-grade heat and hence thermal losses are minimised.The biomethanation can therefore be competitive to raw biogas fed combined heat and power (CHP) systems. Namely, in CHP only about 35-40% of biogas energy is converted into useful electricity. The remainder is obtained in-situ in the form of heat and, except for meeting the needs of digesters heating, most of the in-situ generated heat is often dissipated and wasted. Hence, the CHP systems enable to supply about 40% of raw biogas energy to power grids, i.e. less than half of that supplied by the biomethanation systems to gas grids or for transportation applications. In addition, biomethane can be stored, transported and used flexibly in order to meet fluctuating energy demands. Biomethane is thus a dispatchable sustainable biofuel which can complement the performance of renewable energy systems rich in naturally fluctuating wind and solar power sources. Major uses of biomethane include power-only production, CHP production (but in locations where both power and heat may be sold), vehicle fuel and cooking fuel. These uses require grid injection, fuel tank injection or bottling, i.e. all require compressed biomethane (typical pressure requirement is 20 MPa). In relation to gas compression, CO_2 separation brings benefits associated with reduced gas amount for compression having greater energy density and similar total energy content compared to raw biogas.

Power requirement of different biogas upgrading options is an essential parameter for assessing their technical performance and for achieving the sustainability of biogas. The power requirement of water scrubbing vary depending on plant configuration and pressure used. There are also potentials to reduce power requirement by developing an applying innovative solutions. Therefore, this research has been undertaken to model, analyse and estimate power requirements of various biogas upgrading options including commercial systems. To this aim, models of biogas upgrading for seven plant configurations are implemented, experimentally validated and simulated in order to estimate equipment dimensions, water and air flow rates and other minor operating parameters. Finally, power requirements of these seven plant configurations are calculated, compared and discussed. The paper is thus organised as follows. Section 2 briefly describes the state-of-the-art of biogas upgrading by water scrubbing. Section 3 explains plant configurations that are analysed in the current study. Section 4 introduces models of biogas upgrading and compression while Section 5 summarises simulation procedures. In Section 6 the proposed scrubbing models are validated against experimental data found in literature. Section 7 presents simulation results of upgrading plants. Section 8 provides and compares power requirements for the investigated plant configurations. Section 9 investigates the minimum thermodynamic work and efficiency of biogas upgrading and biomethane compression. Section 10 analyses potential for energy recovery. Finally, Section 11 provides discussions while Section 12 summarises major concluding remarks.

2. State-of-the-art of biogas upgrading by water scrubbing

In recent years, several processes have been developed for the removal of CO_2 and other trace compounds from raw biogas [2-5]. These processes are based on absorption, adsorption, cryogenic or membrane technology [6]. In gas-liquid absorption water can be used as a cheap and environmentally benign solvent for removing CO_2. Water scrubbing makes use of the higher solubility of CO_2 (and H_2S) than the solubility of CH_4 in water. Due to poor CO_2 solubility in water, the CO_2 water absorption rate has to be enhanced. In order to increase CO_2 partial pressure and hence its solubility in the water, the operating pressure of the scrubber is often set between 0.8 and 1.2 MPa. To release the CO_2 from the scrubbing water, and thus to regenerate the water, a second low pressure stripper can be used. In this case, CO_2 is stripped from water at ambient temperature using air as a stripping agent which reduces energy requirements of CO_2 separation compared to other chemical solvents that strongly bind CO_2 and thus require higher stripping temperatures.

Water scrubbing plants are currently operational mainly in Germany and Sweden. According to IEA [7] in 2013 HPWS technology has been employed in 30% upgrading plants in Germany (36 out of 120). Until early 2015 only one company (Malmberg Water AB [8]) completed 42 HPWS plants in Germany and over 80 in Europe. Under incentivisation schemes for biogas [9] existing in some countries, HPWS can be more profitable than electricity from biogas, see e.g. a case study of Italy [10]. This all suggests that the potential for water scrubbing is significant in Europe and likely will be significant beyond Europe.

The state-of-the-art water scrubbing plant configuration is the scrubber-flash-stripper HPWS process, involving CO_2 loaded water flash with gas recycle (see Fig. 1 panel B). In these scrubber-flash-stripper HPWS systems, the raw biogas is compressed to around 0.8 MPa and introduced to the bottom of the scrubber while water is fed to the top of the column. The scrubber packing facilitates contact between the gas and liquid. High purity biomethane leaves the top of the scrubber. Any CH_4 dissolved within the solvent is subsequently separated in a flash tank operating at a reduced pressure of about 0.2 MPa. Released gases that are rich in CH_4 and CO_2 are then returned to the second compressor and mixed with biogas from the first compressor outlet. Biomethane is obtained at the top of the scrubber and sent for drying and further compression (e.g. to around 20 MPa) for grid injection, fuelling station supply or bottling. In most commercial systems, scrubbing water is recirculated following removal of dissolved gases in a stripping column. The stripper is operated at atmospheric pressure and CO_2 is released to the atmospheric air while regenerated water is pumped back to the high pressure scrubber. To ensure smooth work of compressors and packed columns, any particulate matter and condensed moisture are removed from the raw biogas and air streams prior to admitting to the plant. In addition, water filters and CO_2-loaded air biofilters can be applied. In spite of these measures, microbial growth on packing materials is a challenge that may degrade the performance of gas-liquid columns over time [11]

The major deficiency of HPWS is associated with its relatively high power requirements, due to the use of one or more compressor stages for having the scrubbing column pressurised. Since compression raises biogas temperature which would degrade CO_2 solubility, a gas cooling process is therefore required in order to achieve reduced temperature and hence more effective scrubbing with higher CO_2 solubility in water. This all contributes to higher power requirements. Advantages of HPWS are associated with compact scrubber design and less circulating water meaning that CAPEX and OPEX may be lowered.

Instead of enhancing the solubility of CO_2 by raising scrubbing pressure with associated power requirement for biogas compression, CO_2 can be scrubbed under near-atmospheric conditions. Near-atmospheric pressure water scrubbing (NAPWS) does not require biogas compression and cooling, reducing therefore power requirement associated with CO_2 scrubbing. In addition, low pressure columns are cheaper which reduces the CAPEX of NAPWS upgrading plants. However, NAPWS requires a much higher liquid-to-gas ratio due to reduced CO_2 solubility in water under low pressure conditions. The water regeneration step can be achieved by applying a stripping column or a degassing tank. The stripping column in NAPWS systems needs to be larger compared to HPWS systems since more water needs to be circulated and regenerated. The degassing tank stores CO_2-loaded water and enables slow but spontaneous CO_2 degassing to the atmospheric air. Water degassing in a tank is usually less energy intensive but the tank is larger than the stripper. In water degassing, CO_2 desorption is triggered only by the CO_2 concentration difference between the CO_2 vapour pressure present just over the CO_2-loaded water in the tank and CO_2 present in the bulk air. The shortcomings of regenerated NAPWS systems are associated with larger internal water circulation rates with resulting increased power requirement for pumping. In addition, NAPWS systems have higher friction losses associated with energy dissipation occurring when biogas and water are contacted (higher pressure drops). More water in the system means also more water losses by evaporation to raw biogas and stripping air. In addition, in NAPWS systems having larger columns microbiological packing clogging may increase pressure drops and require packing regeneration.

Potentially, the energy intensive water regeneration step can be eliminated in both HPWS and NAPWS systems if cheap water is available. For instance, outlet water from a sewage treatment plant or from river. But in such cases water requirement may be very high, especially in NAPWS plants. Another rarely explored opportunity is associated with using

CO_2-loaded water in aquaculture applications, e.g. farming of algae [12-13], duckweeds [14-15] or azollas [16]. In these applications valorisation of CO_2-loaded water occurs since energy intensive water regeneration is replaced by feeding aquatic plantations. Beneficially, waste biomass from these plantations can be used in anaerobic digestion to increase the amount of produced biogas.

Water scrubbing removes CO_2 from raw biogas but simultaneously it is effective at removing H_2S thus yielding high purity biomethane with a simple biogas purification plant. However, H_2S may be released to stripping air requiring additional treatment of large amounts of air containing diluted H_2S leading high costs per unit of H_2S removed. It is therefore more a disadvantage than an advantage. Potentially, H_2S can be limited in biogas by applying thermophilic anaerobic digestion since higher temperatures are not favourable for sulphuric microorganisms.

Table 1 displays an overview of providers of commercial water scrubbing installations. Basic characteristics of each technology are briefly indicated. However, it needs to be noted that providers reveal very few technical details and hence the detailed comparison of various HPWS installations based only on publicly available information is not possible. Therefore, one of the co-objectives of this study is to evaluate and compare various plant configurations by means of standardised numerical approaches. Such a comparison will be useful in plant selection, design and also in further developing the water scrubbing technology, especially by reducing its power requirement. Table 1 shows that there are a few larger providers as well as a certain number of smaller providers with limited market penetration. The reason is that water scrubbing has a niche market and these few plant providers are sufficient to saturate the market of the European Union. However, there is potential to export these biogas upgrading plants and services beyond Europe where biogas industry is emerging. Most systems shown in Table 1 are scrubber-flash-striper HPWS plants (configuration B in Fig. 1).

Table 1

Providers of commercial scrubber-flash-stripper HPWS plants

Provider	Website	Basic plant characteristics	Operational facilities (2015)
Malmberg Water AB	www.malmberg.se	Malmberg Compact System: claimed upgrading costs 0.01 €/kWh (at 2000 Nm^3/h plant capacity), CH_4 slippage 0.2%, packing plastic rings, oil free compressors to avoid oil leakages to scrubbing water, plant flexibility 50-100% raw biogas input, facilities mainly in Germany, Sweden and UK.	>80
Greenlane Biogas, Flotech, Chesterfield BioGas (Pressure Technologies Group)	www.greenlanebiogas.com, www.flotech.com, www.chesterfieldbiogas.co.uk	Greenlane Water Scrubbing: CH_4 purity 98%, facilities mainly in USA, Canada, Japan, UK, France, Germany, Finland, Spain.	>60
Econet	www.econetgroup.se	Econet: facilities mainly in Sweden.	>15
Ökobit	www.oekobit-biogas.com	Ökobit: methane purity >97% CH_4 content, facilities mainly in Germany.	>7
DMT	www.dmt-et.nl	TS-PHPWS: purity >97 % CH_4 content, CH_4 losses <2%, high efficiency on removal H_2S in one step (<2 ppm in outlet gas), low power consumption (0.4-0.5 kWh/Nm^3 biomethane), facilities in the	>4

		Netherlands, Hungary.	
Schmack Carbotech (Viessmann Group)	www.carbotech.info	Carbotech: claimed upgrading costs 0.01 €/kWh, energy intensity of 0.24 kWh/Nm^3 (at 1000 Nm^3/h raw biogas)	n/a

Notes: n/a - not available

Table 2 compares advantages and disadvantages of water scrubbing in commercial biogas upgrading systems.

Table 2

Advantages and disadvantages of water scrubbing in commercial biogas upgrading systems.

Advantages	**Disadvantages**
High CO_2 separation efficiency (biomethane >97% CH_4)	Packing material clogging due to bacterial growth
Installations are easy in operation and maintenance	Low flexibility toward variation of input raw biogas (50-100%)
Water regeneration by cheap atmospheric air stripping	High power requirement (biogas compression and cooling, water pumping)
Tolerant for trace impurities in biogas	Significant CAPEX (compressors, columns) and OPEX (compressions, pumping)
No need for multiple stages due to favourable equilibria (in contrast to membranes requiring multiple stages)	CO_2-water corrosion issues that may shorten the plant lifetime
Minimal CH_4 slip (in contrast to pressure swing adsorption having significant CH_4 slippage)	
No chemicals (in contrast to chemical/physical scrubbing requiring solvents other than water)	

Reduced corrosion (in contrast to chemical scrubbing sometimes applying corrosive solvents)	
Little environmental emissions of chemicals and their degradation products (in contrast to chemical scrubbing with high adverse environmental impact)	
CO_2-loaded water can be utilised in aquatic plants/algae plantations	

3. Investigated biogas upgrading plant configurations

The current study investigates water scrubbing operated under pressurised (HPWS) and near-atmospheric (NAPWS) conditions in seven upgrading plant configurations as shown in Fig. 1.

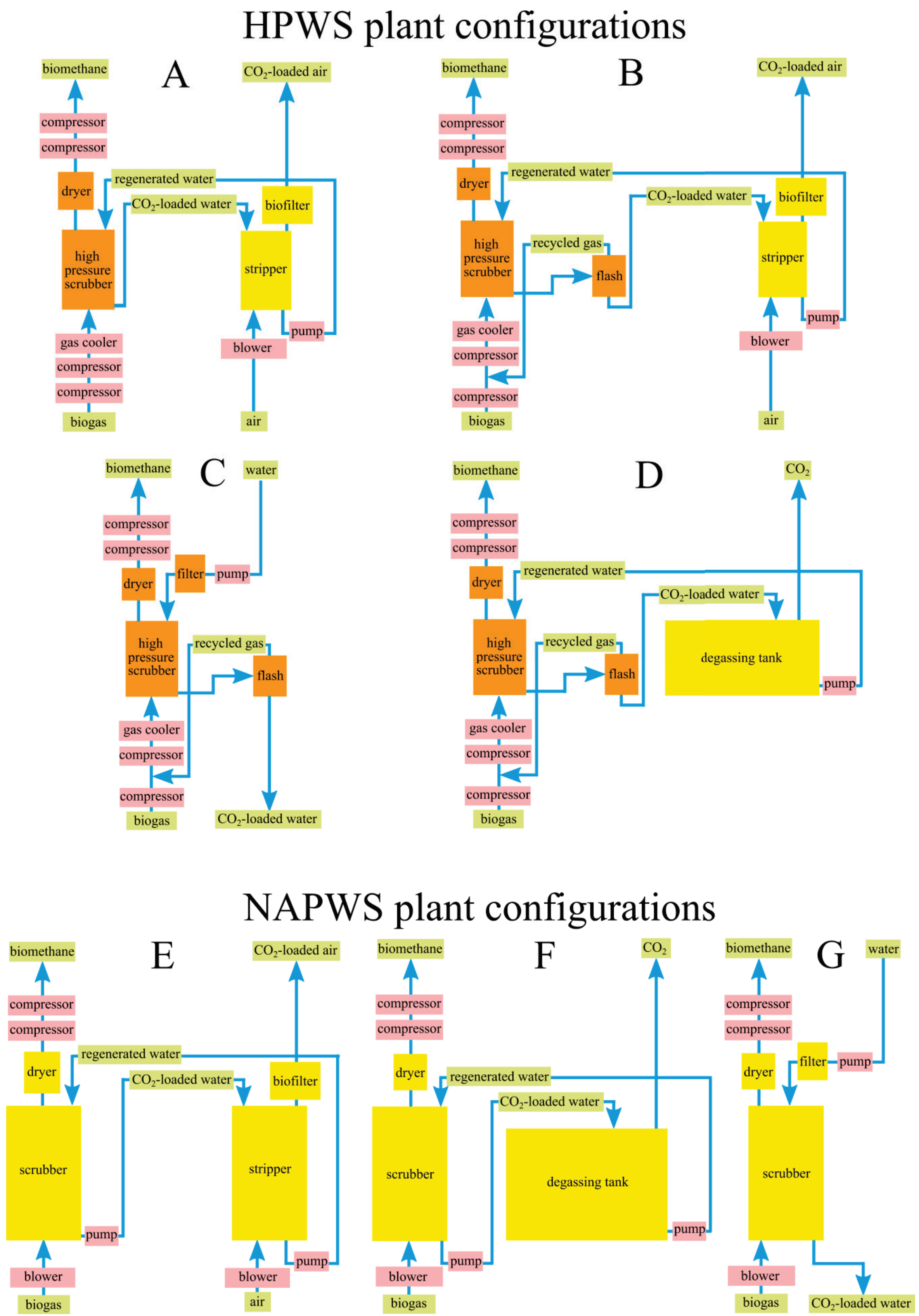

Fig. 1. Schematic of investigated biogas upgrading plant configurations: Panel A - scrubber-stripper HPWS plant, panel B - scrubber-flash-stripper HPWS plant, panel C - scrubber-flash HPWS plant without water

regeneration, panel D - scrubber-flash-degassing tank HPWS plant, panel E - scrubber-stripper NAPWS plant, panel F - scrubber-degassing tank NAPWS plant and panel G - scrubber NAPWS plant without water regeneration. In addition the study analyses plant H (not shown) involving only biogas compression (without upgrading).

HPWS plants are displayed in the panels A-D. The plant presented in the panel A employs water regeneration by air stripping. In the plant B flashing is applied to limit CH_4 slip to the stripping air. In the panel C the presented plant requires cheap water since water regeneration is excluded. The plant in the panel D combines scrubbing, flashing and degassing in a tank. Near-atmospheric pressure (NAPWS) plants are displayed in the panels E-G. The plant configured as shown in the panel E involves a scrubber and an air stripper. The plant configuration in the panel F involves a degassing tank that regenerates water for recirculation without blowing air. The plant G is the most simple but it requires cheap water, for instance, outlet water from a waste water treatment plant. All plant configurations are complemented by biomethane drying and CO_2-loaded air biofiltration (e.g. HEPA filter) to avoid odours and other organic compounds. In addition, raw biogas compression (without upgrading) is considered as a plant in configuration H.

Columns (scrubber and stripper) applied in this study are all packed with suitable materials (ceramic Intalox saddles). This ensures that mass transfer is relatively intensive due to high mass transfer area associated with droplet formation/destruction and film mixing effects. It allows for reduced size of the columns so that power requirements are also lower. Other possible solutions such as falling film or spray absorption gas-liquid contactors have deficiencies. For example falling film contactors are relatively ineffective due to low mass transfer area and low Re numbers thus insufficient turbulence does not intensify mass transfer rates. Spray absorption also has drawbacks because droplets are highly stable and stiff with little internal mixing, especially for viscous solvents which limits mass transfer rates. When a viscous solvent is applied in a spray absorber the mass transfer rate may even decrease with rising solvent concentration, see Table 6 of [17] where with the rise of MEA solvent concentration from 30 to 40 wt% the six fold decrease of CO_2 absorption flux was observed under experimental conditions. For water this effect will be less pronounced, nevertheless still potentially degrading the performance. On the other hand, simple spray or falling film columns are capable of eliminating the problem of microbial growth on the packing.

4. Modelling of biogas upgrading by water scrubbing

4.1. Scrubber and stripper models

The requested column dimensions (diameter and height) and liquid flow rate are related to the characteristics of the biomethane to upgrade (flow rate, concentration), the targeted CO_2 abatement and the effective gas-liquid transfer rate. It is therefore necessary to take into account the relevant transport phenomena to reach reliable estimations of dimensions and operating conditions to ensure.

The governing equations of the scrubber/stripper models derive from the classical one-dimensional modelling approach of packed column working at counter-current. It is considered that both CO_2 and CH_4 can be transferred. Their mass transfer rate, $\tau_{\mathrm{CO_2}}$ and $\tau_{\mathrm{CH_4}}$ respectively, are computed according to the two-film theory [18] by the following expressions [19-20]:

$$\tau_{\mathrm{CO_2}} = M_{\mathrm{CO_2}} \mathcal{A}\, \Omega\, K_{L,\,\mathrm{CO_2}} \left(H_{\mathrm{CO_2}} p_{\mathrm{CO_2},G} - [\mathrm{CO_2}]_L \right) \tag{1}$$

$$\tau_{\mathrm{CH_4}} = M_{\mathrm{CH_4}} \mathcal{A}\, \Omega\, K_{L,\,\mathrm{CH_4}} \left(H_{\mathrm{CH_4}} p_{\mathrm{CH_4},G} - [\mathrm{CH_4}]_L \right) \tag{2}$$

$\mathcal{A}$ is the interfacial area density and Ω is the cross-section area of the column. $M_{\mathrm{CO_2}}$ and $M_{\mathrm{CH_4}}$ are the molar mass of CO_2 and CH_4, $H_{\mathrm{CO_2}}$and $H_{\mathrm{CH_4}}$ are their Henry coefficient and $p_{\mathrm{CO_2},G}$ and $p_{\mathrm{CH_4},G}$ refer to the partial pressure in the gas bulk. It is assumed that the gas follows the Raoult's law and that its total pressure decreases linearly with the vertical position in column according to the pressure drop in the packing. $K_{L,\mathrm{CO_2}}$ and $K_{L,\mathrm{CH_4}}$ are their global mass transfer coefficients. They are derived as classically from the liquid-side and gas-side transfer coefficients. $[\mathrm{CO_2}]_L$ and $[\mathrm{CH_4}]_L$ refer to their molar concentration in liquid bulk.

Thanks to global and species mass balances on an infinitesimal element of column height, the evolution of CO_2 and CH_4 mass fraction x in both phases with the vertical position z can be derived:

$$\frac{d\, x_{\mathrm{CO_2},G}}{dz} = \frac{-\tau_{\mathrm{CO_2}}\left(1 - x_{\mathrm{CO_2},G}\right) + \tau_{\mathrm{CH_4}}\, x_{\mathrm{CO_2},G}}{Q_G} \tag{3}$$

$$\frac{d\, x_{\mathrm{CH_4},G}}{dz} = \frac{-\tau_{\mathrm{CH_4}}\left(1 - x_{\mathrm{CH_4},G}\right) + \tau_{\mathrm{CO_2}}\, x_{\mathrm{CH_4},G}}{Q_G} \tag{4}$$

$$\frac{d\, x_{\mathrm{CO_2},L}}{dz} = \frac{-\tau_{\mathrm{CO_2}}\left(1 - x_{\mathrm{CO_2},L}\right) + \tau_{\mathrm{CH_4}}\, x_{\mathrm{CO_2},L}}{Q_L} \tag{5}$$

$$\frac{d\, x_{\mathrm{CH_4},L}}{dz} = \frac{-\tau_{\mathrm{CH_4}}\left(1 - x_{\mathrm{CH_4},L}\right) + \tau_{\mathrm{CO_2}}\, x_{\mathrm{CH_4},L}}{Q_L} \tag{6}$$

Q_G and $Q_L$are the total gas and liquid mass flow rates, respectively. They are computed locally thanks to the conservations of the inert gas flow rate $\left(1 - x_{\mathrm{CO_2},G} - x_{\mathrm{CH_4},G}\right)Q_G$ and the inert liquid flow rate $(1 - x_{CO_2,L} - x_{CH_4,L})Q_L$. It is worth to mention that the form of these equations differ the classical ones because we consider mass fractions, taking into account the simultaneous CO_2 and CH_4 transfers.

Since CO_2 takes part to reaction in water according to the following equilibria [21-22]:

$$CO_2 + H_2O \rightleftharpoons HCO_3^{\ -} + H^+ \tag{7a}$$

$$HCO_3^{\ -} \rightleftharpoons CO_3^{\ 2-} + H^+ \tag{7b}$$

$$H_2O \rightleftharpoons H^+ + OH^- \tag{7c}$$

$[CO_2]_L$ is not directly related $x_{CO_2,L}$. $[CO_2]_L$ is deduced from $x_{CO_2,L}$ by solving these equilibrium and the electroneutrality equations.

The physico-chemical parameters and the expressions correlating the packing characteristics are found in the literature. Their sources are presented in Table 3.

Table 3

Literature source for the scrubber/stripper models parameters

Type	**Correlation sources**
Mass transfer parameters :	
- characteristics of 25 mm unglazed ceramic Intalox saddle	Table 4.5 and 4.8 in [19]
- column cross section area, pressure drop	Table 4.6 in [19]
- interfacial area density, liquid-side and gas-side transfer coefficients	Table 4.7 in [19], [23]
Henry coefficients :	
- CO_2	[22, 24-25]
- CH_4	[26]

Diffusive coefficients :	
- liquid	
- CO_2	[22, 24]
- CH_4	[27-28], for temperature dependence [29]
- gas	
- CO_2	[30-31]
- CH_4	[32]
Equilibrium constants :	
- Eq. (7a)	[22, 25, 33]
- Eq. (7b)	[25, 34-35]
- Eq. (7c)	[22, 25, 36]

The readers interested in further model details are referred to [37].

4.2. Degassing tank model

The degassing tank used in configurations D and F is a tank with still water in contact with the atmosphere. It is assumed that this tank is perfectly mixed, such that the average CO_2 concentration inside the tank equals the outlet one. At steady-state, its global CO_2 desorption rate is directly derived from the mass balances between its inlet and outlet. The requested interface area of this tank S_{TK} can be deduced by considering a simple gas-liquid transfer equation (similar to Eq. (1)) with most of the transfer resistance in the liquid phase, leading to:

$$S_{\mathrm{TK}} = \frac{Q_L\left(x_{\mathrm{CO_2},L,\,\mathrm{in}} - x_{\mathrm{CO_2},L,\,\mathrm{TK}}\right)}{M_{\mathrm{CO_2}} k_{L,\,\mathrm{TK}}\left(H_{\mathrm{CO_2}} p_{\mathrm{CO_2,air}} - [\mathrm{CO_2}]_{\mathrm{L,\,TK}}\right)} \tag{8}$$

where $p_{CO_2,air}$ the partial pressure of CO_2 in the air and $[CO_2]_{L,TK}$ is the average concentration of CO_2 inside the tank. Concerning the tank mass transfer coefficient $k_{L,TK}$, there are very few correlations in the literature for its estimation. In this work, the value proposed in [38] is used : $k_{L,TK} = 3.4\ 10^{-4}$ m/s.

4.4. Flash tank model

The commercial HPWS plants include a flash tank (see configurations B, C and D). The role of the flash is to minimise losses of methane, since methane is recovered by flashing and gas recycling. This system has been simulated by Cozma et al. [39] but no information regarding energy intensity is provided. In general, the flash raises energy intensity of the HPWS system since a portion of gas needs to be recycled back to the scrubber. In addition, for configuration B and D, a reliable estimation of the characteristics of the liquid leaving the flash tank are important for the scaling and the operating conditions required for liquid regeneration. The flash tank is therefore modelled as a lumped control volume with one liquid inlet and two outlets (gas and liquid) by adopting the following simplifications: (i) ideal phase separation (no liquid entrainment by gas), (ii) vapour and liquid in the flash tank are in thermodynamic equilibrium, (iii) pressure drop inside the flash tank is negligible (p_{TK} is constant), (iv) isothermal and adiabatic flash tank, and (v) water content in vapour is negligible due to the low temperature.

The outlet variables of the flash tank are computed from the inlet ones by solving the governing equations of the proposed model, which include therefore:

$$x_{CO_2,L,in}Q_{L,in} = x_{CO_2,L,out}Q_{L,out} + x_{CO_2,G,out}Q_{G,out} \quad (9)$$

(10)

$$x_{\mathrm{CH_4},L,\mathrm{in}} Q_{L,\mathrm{in}} = x_{\mathrm{CH_4},L,\mathrm{out}} Q_{L,\mathrm{out}} + x_{\mathrm{CH_4},G,\mathrm{out}} Q_{G,\mathrm{out}}$$

(11)

$$\left(1 - x_{\mathrm{CO_2},L,\mathrm{in}} - x_{\mathrm{CH_4},L,\mathrm{in}}\right) Q_{L,\mathrm{in}} = \left(1 - x_{\mathrm{CO_2},L,\mathrm{out}} - x_{\mathrm{CH_4},L,\mathrm{out}}\right) Q_{L,\mathrm{out}}$$

(12)

$$x_{\mathrm{CO_2},G,\mathrm{out}} + x_{\mathrm{CH_4},G,\mathrm{out}} = 1$$

(13)

$$[\mathrm{CO_2}]_{L,\mathrm{out}} = H_{\mathrm{CO_2}}\, p_{\mathrm{CO_2},G,\,\mathrm{out}}$$

(14)

$$[\mathrm{CH_4}]_{L,\mathrm{out}} = H_{\mathrm{CH_4}} p_{\mathrm{CH_4},G,\,\mathrm{out}}$$

4.5. Compressor model

The power requirement of the reciprocating multi-stage compressors (suitable for smaller gas flows typical of biogas plants) is obtained assuming isentropic compression [40] as expressed in eq. below.

$$P_C = \frac{n p_{in} q_G \left(\frac{p_{std}}{p_{in}}\right) \frac{\kappa}{\kappa - 1}\left(\left(\frac{p_{out}}{p_{in}}\right)^{\frac{\kappa-1}{n\kappa}} - 1\right)}{\eta_{CIS}\eta_{CM}} = \frac{n m_G \frac{RT}{M} \frac{\kappa}{\kappa-1}\left(\left(\frac{p_{out}}{p_{in}}\right)^{\frac{\kappa-1}{n\kappa}} - 1\right)}{\eta_{CIS}\eta_{CM}} \quad (15)$$

A reciprocating compressor can achieve a high pressure ratio at comparatively low mass flow rate. It is also relatively cheap. From these reasons reciprocating compressors are typically used in biogas industry.

Two efficiencies are applied: (i) the isentropic efficiency of gas compression (accounting for starting from reversible adiabatic process with no entropy generation) and (ii) the mechanical efficiency (accounting for losses from the seals and valves in the compressor), Table below. Two compression stages are assumed. Equation above is suitable for calculating the power requirement of compressing raw biogas (to 0.8 MPa) and biomethane (to 20 MPa). The ratio of specific heats of biogas (κ) is calculated from the heat capacity at constant pressure and at constant volume of CH_4 and CO_2, depending on their respective concentrations in the biogas or biomethane. The ratio of specific heats can be thus expressed as:

$$\kappa = c_p / c_v \tag{16}$$

4.6. Pump model

The power requirements for pumping regenerated, CO_2-loaded and cooling waters ($P_{P\text{-}RW}$, $P_{P\text{-}LW}$, $P_{P\text{-}COOL}$) are calculated from the water density (ρ_L), gravitational acceleration (g) and liquid flow rate (q_L) as shown below. In order to obtain shaft power, the mechanical efficiency of the pump (η_P) is taken into account.

$$P_P = \rho_L g q_L H_T / \eta_P \tag{17}$$

4.7. Blower model

The power requirement for blowing air (P_B) is calculated from the air density (ρ_A), gravitational acceleration (g) and air flow rate (q_A) as shown below. In order to obtain the shaft power, the mechanical efficiency of the blower (η_B) is assumed to be 60%.

$$P_B = \rho_A g q_A H_T / \eta_B \tag{18}$$

4.8. Gas cooler model

Since biogas scrubbing is more effective when low temperature is maintained in the scrubber (due to the temperature effect on the water CO_2 solubility), the biogas which is heated during compression needs to be cooled. In the current study biogas cooling is designed to reduce its temperature to 5 K above ambient temperature.

The temperature of compressed biogas (T_{out}) is obtained by means of the following equation.

$$T_{out}=T_{in}\left(\frac{p_{out}}{p_{in}}\right)^{\frac{\kappa-1}{\kappa}} \tag{19}$$

The flow rate of cooling water (q_{COOL}) required to cool the biogas is calculated from a simple energy balance.

$$q_{COOL}=\frac{q_G\rho_G c_{PG}(T_{Gout}-T_{Gin})}{\rho_L c_{PL}(T_{Lout}-T_{Lin})} \tag{20}$$

5. Simulation procedures

A typical simulation is realised in several steps. The number and the combination of steps depend on the simulated plant configuration. The simulations are performed using the computational software Matlab. An independent script function correspond to each unit (scrubber, flash, ...). These functions are called by a master script, depending on the considered configuration.

Except for the model validation (for which the simulation are compared to experiments on columns with given diameter and height), the simulations of the scrubber and stripper models are preceded by their size estimation.

For the scrubber, the mass flow rate and the CO_2 fraction at inlet and the targeted CO_2 fraction at the outlet enables the calculation of the global CO_2 transfer rate (along the whole column). This serves to estimate the necessary liquid flow rate. Once it is known, the column diameter is then calculated for the corresponding superficial velocities in the used packing (25 mm unglazed ceramic Intalox saddle), such that the superficial gas velocity corresponds to 60% of the flooding one. After this stage, the minimum height matching the inlet and outlet criteria, is roughly estimated by solving the model equations, starting from the bottom to the top of the column, using the *ode15s* routine. The height such that the CO_2 mass fraction matches the targeted one is then the requested column height. Using the identified diameter and height, the boundary value problem is solved again using the *bvp4c* routine to accurately compute the actual outlet variables according to the inlet ones.

The same procedure is used for the stripper but in this case the outlet target is replaced by the CO_2 fraction in the injected air, which is closed to 0.04% in mole.

The tank free interface area is computed immediately using Eq. (8), whereas the equation system Eqs. (9)-(11) describing the flash tank is solved using the *fsolve* routine. Note that for configuration involving the flash tank (B,C,D), the scrubber function and the flash function are executed several times to ensure the convergence of the outlet variable.

Concerning the compressor, pump, blower, and gas cooler, the maximum pressure ratio is 4. It determined the number of compressing stages. The power requirement was directly calculated using equations provided in Section 4.

6. Validation of the biogas upgrading plant model

The model is validated by using experimental results obtained by different authors in order to minimise the risk of using incorrect or misleading data. Simulation results are compared to experimental data and average deviations are calculated. Fig. 2 panel A compares CO_2 removal from biogas for a range of different biogas upgrading plants. The CO_2 removal from biogas is defined as follows:

$$\eta_{CO2} = \frac{x_{CO2,G,in,SCR} - x_{CO2,G,out,SCR}}{x_{CO2,G,in,SCR}} 100\% \quad (21)$$

Fig. 2 panel B presents the comparison of experimental and simulated molar fraction of CO_2 in biomethane ($x_{CO_2,G,out,SCR}$).

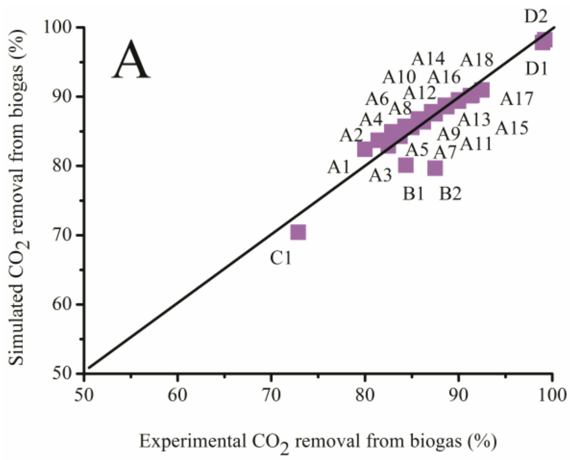

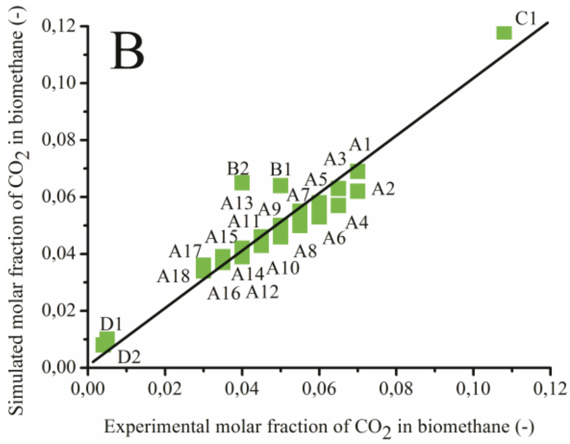

Fig. 2. Comparison of experimental and simulated results for various biogas upgrading plants. Panel A - CO_2 removal from biogas, panel B - molar fraction of CO_2 in biomethane. Experimental data were taken from A [41-42], B [43], C [44], and D [45]. Detailed parameters: A - $p_{G,in,SCR}$ = 1 MPa, $\mathcal{D}_{SCR}$ = 0.15 m, $\mathcal{H}_{SCR}$ = 3.0 m, $\mathcal{Q}_{G,in,SCR}$ = 20.0 m^3/h, $x_{CO_2,G,out,SCR}$ = 0.070; points: A1 - $\mathcal{Q}_{L,in,SCR}$ = 1.00 kg/s, $x_{CO_2,G,in,SCR}$ = 0.40, $x_{CO_2,G,out,SCR}$ = 0.070; A2 - $\mathcal{Q}_{L,in,SCR}$ = 1.00 kg/s, $x_{CO_2,G,in,SCR}$ = 0.35, $x_{CO_2,G,out,SCR}$ = 0.070; A3 - $\mathcal{Q}_{L,in,SCR}$ = 1.03 kg/s, $x_{CO_2,G,in,SCR}$ = 0.40, $x_{CO_2,G,out,SCR}$ = 0.065; A4 - $\mathcal{Q}_{L,in,SCR}$ = 1.03 kg/s, $x_{CO_2,G,in,SCR}$ = 0.35, $x_{CO_2,G,out,SCR}$ = 0.065; A5 - $\mathcal{Q}_{L,in,SCR}$ = 1.06 kg/s, $x_{CO_2,G,in,SCR}$ = 0.40, $x_{CO_2,G,out,SCR}$ = 0.060, A6 - $\mathcal{Q}_{L,in,SCR}$ = 1.06 kg/s, $x_{CO_2,G,in,SCR}$ = 0.35, $x_{CO_2,G,out,SCR}$ = 0.060; A7 - $\mathcal{Q}_{L,in,SCR}$ = 1.08 kg/s, $x_{CO_2,G,in,SCR}$ = 0.40, $x_{CO_2,G,out,SCR}$ = 0.055; A8 - $\mathcal{Q}_{L,in,SCR}$ = 1.08 kg/s, $x_{CO_2,G,in,SCR}$ = 0.35, $x_{CO_2,G,out,SCR}$ = 0.055; A9 - $\mathcal{Q}_{L,in,SCR}$ = 1.11 kg/s, $x_{CO_2,G,in,SCR}$ = 0.40, $x_{CO_2,G,out,SCR}$ = 0.050; A10 - $\mathcal{Q}_{L,in,SCR}$ = 1.11 kg/s, $x_{CO_2,G,in,SCR}$ = 0.35, $x_{CO_2,G,out,SCR}$ = 0.050; A11 - $\mathcal{Q}_{L,in,SCR}$ = 1.14 kg/s, $x_{CO_2,G,in,SCR}$ = 0.40, $x_{CO_2,G,out,SCR}$ = 0.045; A12 - $\mathcal{Q}_{L,in,SCR}$ = 1.14 kg/s, $x_{CO_2,G,in,SCR}$ = 0.35, $x_{CO_2,G,out,SCR}$ = 0.045; A13 - $\mathcal{Q}_{L,in,SCR}$ = 1.17 kg/s, $x_{CO_2,G,in,SCR}$ = 0.40, $x_{CO_2,G,out,SCR}$ = 0.040; A14 - $\mathcal{Q}_{L,in,SCR}$ = 1.17 kg/s, $x_{CO_2,G,in,SCR}$ = 0.35, $x_{CO_2,G,out,SCR}$ = 0.040; A15 - $\mathcal{Q}_{L,in,SCR}$ = 1.19 kg/s, $x_{CO_2,G,in,SCR}$ = 0.40, $x_{CO_2,G,out,SCR}$ = 0.035; A16 - $\mathcal{Q}_{L,in,SCR}$ = 1.19 kg/s, $x_{CO_2,G,in,SCR}$ = 0.35, $x_{CO_2,G,out,SCR}$ = 0.035; A17 - $\mathcal{Q}_{L,in,SCR}$ = 1.22 kg/s, $x_{CO_2,G,in,SCR}$ = 0.40, $x_{CO_2,G,out,SCR}$ = 0.030; A18 - $\mathcal{Q}_{L,in,SCR}$ = 1.22 kg/s, $x_{CO_2,G,in,SCR}$ = 0.35, $x_{CO_2,G,out,SCR}$ = 0.030; B - $\mathcal{D}_{SCR}$ = 0.15 m, $\mathcal{H}_{SCR}$ = 3.5 m, $\mathcal{Q}_{G,in,SCR}$ = 1.0 m^3/h, $\mathcal{Q}_{L,in,SCR}$ = 0.42 kg/s, $x_{CO_2,G,in,SCR}$ = 0.32; points: B1 - $p_{G,in,SCR}$ = 0.8 MPa, $x_{CO_2,G,out,SCR}$ = 0.050; B2 - $p_{G,in,SCR}$ = 1 MPa, $x_{CO_2,G,in,SCR}$ = 0.32, $x_{CO_2,G,out,SCR}$ = 0.040; C - point: C1 - $p_{G,in,SCR}$ = 0.3 MPa, $\mathcal{D}_{SCR}$ = 0.1 m, $\mathcal{H}_{SCR}$ = 1.0 m, $\mathcal{Q}_{G,in,SCR}$ = 0.3 m^3/h, $\mathcal{Q}_{L,in,SCR}$ = 0.3 kg/s, $x_{CO_2,G,in,SCR}$ = 0.40, $x_{CO_2,G,out,SCR}$ = 0.108; D - $p_{G,in,SCR}$ = 0.8 MPa, $\mathcal{D}_{SCR}$ = 0.1 m, $\mathcal{H}_{SCR}$ = 1.0 m, $\mathcal{Q}_{G,in,SCR}$ = 242.3 m^3/h; points: D1 - $\mathcal{Q}_{L,in,SCR}$ = 13.3 kg/s, $x_{CO_2,G,out,SCR}$ = 0.0047, p_{FLS} = 0.3 MPa; D2 - $\mathcal{Q}_{L,in,SCR}$ = 12.06 kg/s, $x_{CO_2,G,out,SCR}$ = 0.0036, p_{FLS} = 0.4 MPa.

For the presented set of data average deviation is 1.7% for CO_2 removal from biogas and 14.7% for molar fraction of CO_2 in biomethane. The distribution of points in Figure 2 on both sides of the line means that the model well predicts average behaviour of the system obtained in experimental conditions. This suggests that the employed models are capable of predicting CO_2 separation.

Other simulation results are similar to those obtained by [46] where specific power requirement of 0.21 kWh/Nm^3 was reported for a plant in configuration B upgrading 500 Nm^3/h raw biogas which is roughly the same as our predictions. In an upgrading plant in configuration B processing 500 Nm^3/h of raw biogas we obtained water circulation rate of 24.8 kg/s (at 283.15 K) while [46] reported 25.7 kg/s. Consequently, the constructed models are considered sufficiently validated for energy efficiency analyses of this work.

7. Simulation results of upgrading plants

The constructed and validated models are subsequently simulated to yield equipment dimensions, water/air flow rates and other operational biogas upgrading plant parameters.

For all cases, the column diameter is estimated such that it leads to liquid and gas flow rates corresponding to 60 % of the flooding rate. All configuration simulations are realised considering a 250 Nm^3/h biomethane stream to upgrade at 288.15 K, with CO_2 and CH_4 molar fraction of 0.34 and 0.62, respectively. The treated gas has to achieve a CO_2 depletion such that the outlet CO_2 molar fraction is 0.02.

To close the equation system, some supplementary conditions have to be imposed, depending on the considered configuration:

- the mass fraction of absorbed CO_2 in the liquid leaving the scrubber is set in all configurations to a value corresponding to 75 % of the one at equilibrium with the entering gaseous phase (i.e. bottom). It depends thus on the values of the total pressure and the CO2 mass fraction at the inlet of the scrubber and on the presence of the flash tank. It ensures an always positive transfer driving force at the scrubber bottom.
- for the configuration with a liquid regeneration (A, B, D, E and F), the regenerated liquid entering in the scrubber has a mass fraction corresponding to 20 times the mass fraction at equilibrium with atmosphere at 288.15 K.
- for the configuration equipped with a stripper (A, B and E), the reached CO_2 mass fraction at the gas outlet is imposed as a fraction of the equilibrium value with the liquid entering in the stripper. It can be higher in low pressure configuration than in high pressure configuration. 0.5 times the equilibrium value is used for configuration E (low pressure) and 0.25 times for configurations A and B (high pressure).

Using this approach, it is possible to compare the various configurations, with the same feed and the same target, and some adjustable parameters. Simulations results for all tested configurations are presented in Tables 4-6.

Table 4
Simulation results for all investigated upgrading plant configurations. Operating parameters: scrubber inlet pressure $p_{G,\mathrm{in,SCR}}$ = 8 10^5 Pa; stripper inlet pressure $p_{G,\mathrm{in,STR}}$ = 1.2 10^5 Pa; flash pressure 2.02 10^5 Pa; biogas volumetric flow rate 250 Nm^3/h; biogas composition yCO_2=0.35, yCH_4=0.649, y_{INERT}=0.001; biomethane composition (approximately) yCO_2=0.02, yCH_4=0.98; operating temperature T=288.15K; biogas inlet pressure p=0.1013 MPa; packing - ceramic Intalox saddle; the ratio of gas flow rate to flooding gas flow rate = 0.6; tank transfer coefficient $k_{L,\mathrm{TK}}$=3.4 10^{-4} m/s; pressure above degassing tank p_{TK} = 1 atm; the ratio of the mass fraction of absorbed CO_2 in the liquid leaving the scrubber to the mass fraction at equilibrium with the entering gaseous phase Abso.feqCO2_out=0.75; the ratio of the reached CO_2 mass fraction at the gas outlet to the mass fraction at equilibrium with the liquid entering in the stripper Deso.feqCO2_out=0.5 (for configuration E (low pressure)), Deso.feqCO2_out=0.25 (for configurations A and B (high pressure)).

CO_2 mass fraction in water at scrubber outlet	CO_2 mass fraction in water at scrubber inlet	CO_2 mass fraction in water at stripper outlet	Water flow rate in scrubber	Scrubber diameter	Scrubber height	Stripper diameter	Stripper height	Air flow rate in stripper	Air flow rate in stripper	Flash recovery	Gas flow rate from flash	Tank surface area	Pressure at scrubber inlet	Pressure in flash tank	CH_4 slip	Pressure drop in scrubber	Pressure drop in stripper	Configuration
$x_{CO_2,L,\mathrm{out,SC}}$	$x_{CO_2,L,\mathrm{in,SCR}}$	$x_{CO_2,G,\mathrm{out,ST}}$	$Q_{L,\mathrm{in,SCR}}$	$\mathcal{D}_{\mathrm{SCR}}$	$\mathcal{H}_{\mathrm{SCR}}$	$\mathcal{D}_{\mathrm{STR}}$	$\mathcal{H}_{\mathrm{STR}}$	$Q_{G,\mathrm{in,STR}}$	$Q_{G,\mathrm{in,STR}}$	α_{FLS}	$Q_{G,\mathrm{out,FL}}$	S_{TK}	$p_{G,\mathrm{in,SCR}}$	p_{FLS}	η_{CH4}	Δp	Δp	
-	-	-	(kg/s)	(m)	(m)	(m)	(m)	(kg/s)	(Nm^3/h)	(%)	(kg/s)	(m^2)	(MPa)	(MPa)	(%)	(Pa)	(Pa)	
3.90e-3	1.50e-5	0.617	11.93	0.71	7.13	0.71	13.26	2.85e-2	79.4	-	-	-	0.8	-	3.78	2374	5009	A
4.80e-3	1.50e-5	0.536	14.30	0.78	6.80	0.78	11.35	4.00e-2	111.4	98.15	2.30e-2	-	0.8	0.202	0.21	2201	3734	B
4.80e-3	7.50e-7	-	14.24	0.78	6.71	-	-	-	-	98.16	2.30e-2	-	0.8	0.202	0.21	2163	-	C
4.80e-3	1.50e-5	-	14.29	0.78	6.81	-	-	-	-	98.15	2.29e-2	9230	0.8	0.202	0.21	2204	-	D
5.81e-4	1.50e-5	0.22	81.56	1.94	6.98	1.85	12.15	1.66e-1	462.0	-	-	-	0.12	-	3.88	5425	5270	E
5.81e-4	1.50e-5	-	81.48	1.94	6.91	-	-	-	-	-	-	9217	0.12	-	3.87	5372	-	F
5.80e-4	7.50e-7	-	79.48	1.91	6.36	-	-	-	-	-	-	-	0.12	-	3.75	4839	-	G

Table 5

Simulation results for all investigated upgrading plant configurations. Operating parameters: scrubber inlet pressure $p_{G,\text{in,SCR}}$ = 8 10^5 Pa; stripper inlet pressure $p_{G,\text{in,STR}}$ = 1.2 10^5 Pa; flash pressure 2.02 10^5 Pa; biogas volumetric flow rate 250 Nm^3/h; biogas composition yCO_2=0.35, yCH_4=0.649, y_{INERT}=0.001; biomethane composition (approximately) yCO_2=0.02, yCH_4=0.98; operating temperature T=283.15K; biogas inlet pressure p=0.1013 MPa; packing - ceramic Intalox saddle; the ratio of gas flow rate to flooding gas flow rate = 0.6; tank transfer coefficient $k_{L,\text{TK}}$=3.4 10^{-4} m/s; pressure above degassing tank p_{TK} = 1 atm; the ratio of the mass fraction of absorbed CO_2 in the liquid leaving the scrubber to the mass fraction at equilibrium with the entering gaseous phase Abso.feqCO2_out=0.75; the ratio of the reached CO_2 mass fraction at the gas outlet to the mass fraction at equilibrium with the liquid entering in the stripper Deso.feqCO2_out=0.5 (for configuration E (low pressure)), Deso.feqCO2_out=0.25 (for configurations A and B (high pressure)).

CO_2 mass fraction in water at scrubber outlet	CO_2 mass fraction in water at scrubber inlet	CO_2 mass fraction in water at stripper outlet	Water flow rate in scrubber	Scrubber diameter	Scrubber height	Stripper diameter	Stripper height	Air flow rate in stripper	Air flow rate in stripper	Flash recovery	Gas flow rate from flash	Tank surface area	Pressure at scrubber inlet	Pressure in flash tank	CH_4 slip	Pressure drop in scrubber	Pressure drop in stripper	Configuration
$x_{CO_2,L,\text{out,SC}}$	$x_{CO_2,L,\text{in,SCR}}$	$x_{CO_2,G,\text{out,ST}}$	$Q_{L,\text{in,SCR}}$	$\mathcal{D}_{\text{SCR}}$	$\mathcal{H}_{\text{SCR}}$	$\mathcal{D}_{\text{STR}}$	$\mathcal{H}_{\text{STR}}$	$Q_{G,\text{in,STR}}$	$Q_{G,\text{in,STR}}$	α_{FLS}	$Q_{G,\text{out,FL}}$	S_{TK}	$p_{G,\text{in,SCR}}$	p_{FLS}	η_{CH4}	Δp	Δp	
-	-	-	(kg/s)	(m)	(m)	(m)	(m)	(kg/s)	(Nm^3/h)	(%)	(kg/s)	(m^2)	(MPa)	(MPa)	(%)	(Pa)	(Pa)	
4.70e-3	1.83e-5	0.619	9.69	0.64	7.79	0.64	14.42	2.83e-2	78.9	-	-	-	0.8	-	2.63	2200	4634	A
5.30e-3	1.70e-5	0.543	12.39	0.73	7.27	0.73	12.13	3.88e-2	108.0	98.48	2.09e-2	-	0.8	0.202	0.15	2130	3654	B
5.40e-3	8.48e-7	-	12.33	0.72	7.14	-	-	-	-	98.51	2.11e-2	-	0.8	0.202	0.15	2084	-	C
5.40e-3	1.70e-5	-	12.37	0.73	7.25	-	-	-	-	98.50	2.11e-2	8107	0.8	0.202	0.15	2122	-	D
6.60e-4	1.70e-5	0.22	71.71	1.80	7.32	1.74	12.45	1.65e-1	460.4	-	-	-	0.12	-	3.09	5134	4878	E
6.60e-4	1.70e-5	-	71.70	1.80	7.30	-	-	-	-	-	-	8080	0.12	-	3.09	5124	-	F
6.57e-4	8.48e-7	-	69.95	1.77	6.74	-	-	-	-	-	-	-	0.12	-	3.00	4634	-	G

Table 6

Simulation results for all investigated upgrading plant configurations. Operating parameters: scrubber inlet pressure $p_{G,\mathrm{in,SCR}}$ = 8 10^5 Pa; stripper inlet pressure $p_{G,\mathrm{in,STR}}$ = 1.2 10^5 Pa; flash pressure 2.02 10^5 Pa; biogas volumetric flow rate 1000 Nm^3/h; biogas composition yCO_2=0.35, yCH_4=0.649, y_{INERT}=0.001; biomethane composition (approximately) yCO_2=0.02, yCH_4=0.98; operating temperature T=288.15K; biogas inlet pressure p=0.1013 MPa; packing - ceramic Intalox saddle; the ratio of gas flow rate to flooding gas flow rate = 0.6; tank transfer coefficient $k_{L,\mathrm{TK}}$=3.4 10^{-4} m/s; pressure above degassing tank p_{TK} = 1 atm; the ratio of the mass fraction of absorbed CO_2 in the liquid leaving the scrubber to the mass fraction at equilibrium with the entering gaseous phase Abso.feqCO2_out=0.75; the ratio of the reached CO_2 mass fraction at the gas outlet to the mass fraction at equilibrium with the liquid entering in the stripper Deso.feqCO2_out=0.5 (for configuration E (low pressure)), Deso.feqCO2_out=0.25 (for configurations A and B (high pressure)).

CO_2 mass fraction in water at scrubber outlet	**CO_2 mass fraction in water at scrubber inlet**	**CO_2 mass fraction in water at stripper outlet**	**Water flow rate in scrubber**	**Scrubber diameter**	**Scrubber height**	**Stripper diameter**	**Stripper height**	**Air flow rate in stripper**	**Air flow rate in stripper**	**Flash recovery**	**Gas flow rate from flash**	**Tank surface area**	**Pressure at scrubber inlet**	**Pressure in flash tank**	**CH_4 slip**	**Pressure drop in scrubber**	**Pressure drop in stripper**	**Configuration**
$x_{CO_2,L,\mathrm{out,SC}}$	$x_{CO_2,L,\mathrm{in,SCR}}$	$x_{CO_2,G,\mathrm{out,ST}}$	$\mathcal{Q}_{L,\mathrm{in,SCR}}$	$\mathcal{D}_{\mathrm{SCR}}$	$\mathcal{H}_{\mathrm{SCR}}$	$\mathcal{D}_{\mathrm{STR}}$	$\mathcal{H}_{\mathrm{STR}}$	$\mathcal{Q}_{G,\mathrm{in,ST}}$	$\mathcal{Q}_{G,\mathrm{in,ST}}$	α_{FLS}	$\mathcal{Q}_{G,\mathrm{out,FL}}$	S_{TK}	$p_{G,\mathrm{in,SCR}}$	p_{FLS}	η_{CH4}	Δp	Δp	
-	**-**	**-**	**(kg/s)**	**(m)**	**(m)**	**(m)**	**(m)**	**(kg/s)**	**(Nm^3/h)**	**(%)**	**(kg/s)**	**(m^2)**	**(MPa)**	**(MPa)**	**(%)**	**(Pa)**	**(Pa)**	
3.90e-3	1.50e-5	0.617	47.70	1.42	7.12	1.42	13.26	1.14e-1	317.5	-	-	-	0.8	-	3.78	2371	5008	A
4.80e-3	1.50e-5	0.536	57.32	1.56	6.83	1.56	11.35	1.60e-1	446.7	98.15	9.24e-2	-	0.8	0.202	0.21	2212	3736	B
4.80e-3	7.48e-7	-	57.12	1.55	6.69	-	-	-	-	98.19	9.47e-2	-	0.8	0.202	0.21	2156	-	C
4.80e-3	1.50e-5	-	57.13	1.55	6.83	-	-	-	-	98.15	9.24e-2	37006	0.8	0.202	0.21	2213	-	D
5.81e-4	1.50e-5	0.22	325.63	3.87	6.86	3.71	12.14	6.62e-1	1844.81	-	-	-	0.12	-	3.87	5324	5269	E
5.81e-4	1.50e-5	-	325.63	3.87	6.86	-	-	-	-	-	-	36886	0.12	-	3.87	5323	-	F
5.81e-4	7.48e-7	-	317.79	3.81	6.34	-	-	-	-	-	-	-	0.12	-	3.75	4818	-	G

8. Power requirements of biogas upgrading in various plants configurations

Power requirements of the upgrading process depend on plant configurations and plant operating parameters such as scrubbing pressure and temperature. This study investigates 7 plant configurations involving two scrubbing pressures (Fig. 1) and one plant relying on raw biogas compression (without upgrading). The investigated plants are simulated and optimised by employing engineering know-how available in open literature and industrial practice. For example, optimal scrubbing pressure for which minimal power requirement can be obtained is about 0.8 MPa while flashing pressure is typically set at 0.2 MPa [41]. Temperatures vary between winters and summers and depend on regional climate. Here we test 288.15 K and 283.15 K. Several operating parameters are retrieved during simulations to meet design targets such as biomethane purity, methane slip or pressure drop. For these optimised operating conditions power requirements are calculated and compared.

Upgrading plants need power for compressing raw biogas in order to raise the pressure in the scrubber ($PR_{C\text{-}BG}$). Water is circulated in most configurations by involving pumps and power requirements associated with pumping regenerated water ($PR_{P\text{-}RW}$) and CO_2-loaded water ($PR_{P\text{-}LW}$) are usually remarkable. Water is also needed to cool the compressed biogas prior to entering the scrubber for gas-liquid absorption ($PR_{P\text{-}COOL}$). Another contribution is associated with blowing air to strip CO_2 from CO_2-loaded water ($PR_{B\text{-}A}$). Additional power requirements include the control of valves and the contribution from auxiliary equipment such as a dryer or a filter and they are treated collectively as baseload power ($PR_{BASELOAD}$). The total power requirement of an upgrading plant (PR_T^{BM}) can therefore be expressed as:

$$PR_T^{BM} = PR_{C-BG} + PR_{P-RW} + PR_{P-LW} + PR_{P-COOL} + PR_{B-A} + PR_{BASELOAD} \quad (22)$$

The obtained biomethane is usually further compressed to high pressure (typically 20 MPa) ($PR_{C\text{-}BM}$) and this contribution adds to the total power requirement (PR_T^{CBM}):

$$PR_T^{CBM}=PR_T^{BM}+PR_{C-BM} \tag{23}$$

Various power consumptions are calculated using adequate expressions. The total pressure head (H_T) is needed to calculate pumping and blowing power. It is calculated as the sum of the pressure difference (H_{SCR} - H_{ATM}), and the static (H_S) and dynamic (H_D) heads as shown below.

$$H_T=H_S+H_D+(H_{SCR}-H_{ATM}) \tag{24}$$

The static head is taken equal to the height of the scrubber. The dynamic head is calculated from the Darcy-Weisbach equation:

$$H_D=f\frac{L}{D}\frac{w^2}{2g} \tag{25}$$

Friction factor f is obtained explicitly from a relationship approximating the Colebrook-White equation [47].

$$f=\frac{6.4}{\left(ln(Re)-ln\left(1+0.01Re\frac{\varepsilon}{D}\left(1+10\sqrt{\frac{\varepsilon}{D}}\right)\right)\right)^{2.4}} \tag{26}$$

The pressure difference H_{SCR} - H_{ATM} is obtained by subtracting the pressure in the scrubber and the atmospheric pressure.

Table 7 provides assumptions made in calculations of required power.

Table 7

Assumptions made in calculations of the power requirements.

Variable	**Value**	**Reference**
pump efficiency (η_P)	60%	this study
adiabatic expansion coefficient - heat capacity ratio (κ)	1.306 (CH_4), 1.293 (CO_2), 1.301 (biogas 65% CH_4), 1.306 (biomethane >98% CH_4)	[48]
compressor isentropic efficiency (η_{CIS})	75%	[40]
compressor mechanical efficiency (η_{CM})	80%	[40]
rotary hydraulic pumping device efficiency (RHPD) (η_{RHPD})	70%	[49]
water pipe velocity (w)	2.5 m/s	this study
water pipe length (L), including head loss from water pipe bends	8-16m depending on configuration	this study
pipe roughness (ε)	0.0002 (other examples: PVC 0.0001 m (averaged over lifetime) (new 0.000005 m) steel 0.00015 m (averaged over lifetime) (new 0.00006 m))	this study

Since the solubility of CH_4 in water is about 3% that of CO_2 a part of methane is washed out from biogas. Therefore a flash tank needs to be used downstream to the scrubber in order to minimise CH_4 slip in the stripper where methane is transferred to stripping air. When the pressure of CO_2-loaded water is decreased in the flash tank, most of CH_4 is released to the gas phase and is recompressed and recycled back to the scrubber. The flashing tank in this study is assumed to operate at a pressure of about 0.2 MPa. In HPWS systems the flashing tank and stripper are fed with pressurised water and there is no additional power requirement for pumping water. However, in the NAPWS systems the scrubber and stripper operate under near-atmospheric pressure and additional energy is required to pump water to the top of the stripper or degassing tank.

In addition, some baseload power is required ($P_{BASELOAD}$). 500-750 W is assumed to be needed for the control valves operation while 0-200 W is assumed to be needed in auxiliary components such as a dryer or a biofilter. These minor components are not included in the model and their contributions are evaluated through the baseload power.

Each of calculated power requirements is subsequently expressed as specific power requirements (power requirement per volumetric flow rate of raw biogas):

$$SPR = \frac{PR}{V_{BG}} \tag{27}$$

Finally, two aggregate specific power requirements are calculated for all plant configurations. The first is the specific power requirement of the entire biogas upgrading plant:

$$SPR^{BM} = \frac{P_T^{BM}}{V_{BG}} \tag{28}$$

The second is specific power requirement of the biogas upgrading plant followed by biomethane compression.

$$SPR^{CBM} = \frac{P_T^{CBM}}{V_{BG}} \tag{29}$$

Moreover, in order to enable more in-depth insights into the plant operation specific power requirements are calculated for each unit operation and/or upgrading plant component. The results are presented in Figs. 3 and 4. Fig. 3 compares specific power requirements of various biogas upgrading plants analysed in this study including contributions from all meaningful unit operations and/or upgrading plant components.

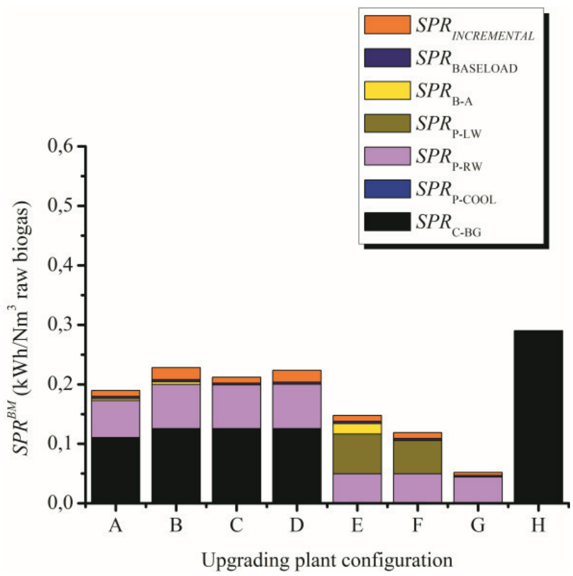

Fig. 3. Specific power requirements of various investigated biogas upgrading plants (SPR^{BM}) including contributions from all meaningful unit operations and/or upgrading plant components. Parameters: raw biogas flow rate 250 Nm^3/h, $T = 288.15$ K.

From Fig. 3 it is seen that the lowest specific power requirement is obtained by applying NAPWS plants without water regeneration (0.05 kWh/Nm^3 raw biogas) but this plant requires cheap water supply, e.g. outlet water from a sewage treatment plant. All HPWS plants have specific power requirements between 0.18 and 0.21 kWh/Nm^3 raw biogas. Other NAPWS plants have specific power requirements between 0.11 and 0.14 kWh/Nm^3 raw biogas. Biogas compression without upgrading requires 0.29 kWh/Nm^3 raw biogas.

Fig. 4 displays specific power requirements of tested plant configurations including biogas upgrading and biomethane compression along with contributions from all unit operations and/or plant components.

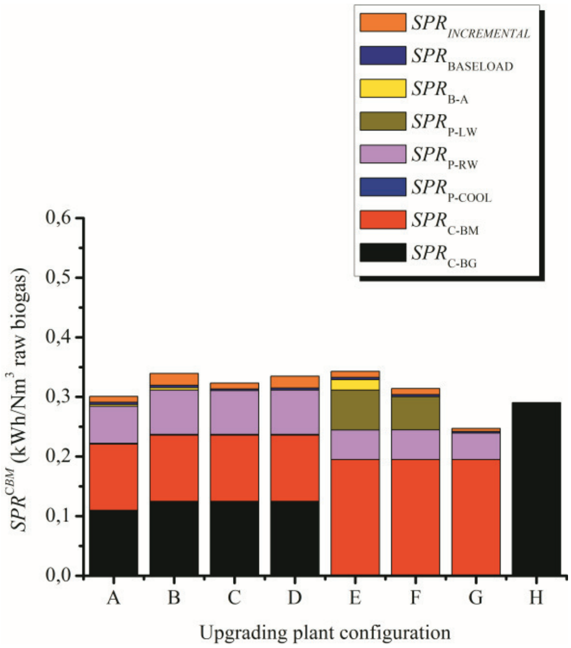

Fig. 4. Specific power requirements of various biogas upgrading plants followed by biomethane compression (SPR^{CBM}) including contributions from all meaningful unit operations and/or upgrading plant components.. Parameters: raw biogas flow rate 250 Nm^3/h, T = 288.15 K.

From Fig. 4 it can be observed that the specific power requirement of biomethane compression to 20 MPa adds about 0.11 kWh/Nm^3 raw biogas for HPWS plants and 0.19 kWh/Nm^3 raw biogas for NAPWS plants. Overall HPWS plants are slightly superior if compressed biomethane is the target, except the situation if cheap water is available (from waste water treatment plant or river).

8.1. Impact of temperature on power requirements

Fig. 5 explains how operating temperature reduction from 288.15 to 283.15 K affects the specific power requirements of investigated plants. It is seen that at temperatures reduced by 5 K (1.7%) *SPR* is decreased by up to about 0.015 kWh/Nm^3 raw biogas (about 4-5%). For HPWS plants, the most remarkable reduction is due to pumping regenerated water since at lower temperatures less water is required to absorb CO_2 (increased solubility effect). The magnitude of reduction is about 0.01 kWh/Nm^3 raw biogas for configurations A-F and half of that for configuration G. For NAPWS plants also less water is circulated and reductions in *SPR* are observed both for regenerated water and CO_2 loaded water. Besides, some *SPR* reduction is also found in compressing biogas and biomethane, about 0.005 kWh/Nm^3 raw biogas for all tested configurations.

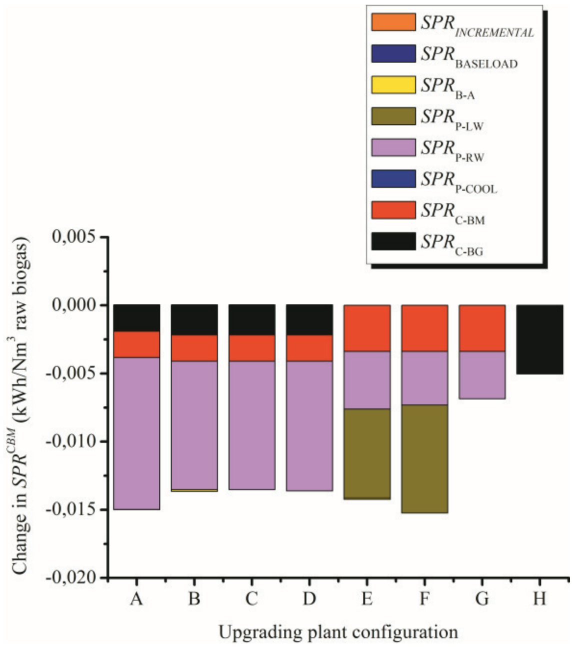

Fig. 5. Impact of reduced operating temperature on the specific power requirements of various investigated biogas upgrading plants followed by biomethane compression (SPR^{CBM}). Parameters: raw biogas flow rate 250 Nm^3/h, T=283.15 vs. 288.15 K.

These obtained results have geographical implications. Namely, the reduction in *SPR* achieved at lower temperatures means that more favourable conditions for biogas upgrading exist in moderate and cold climates. The *SPR* reduction is due to lower scrubbing temperature, increased CO_2 solubility in water, less required circulating solvent, and reduced gas compression work. For hot climates this technology is less suitable due to remarkable power requirements for cooling which is normally not needed or can be avoided in cold climates. For example, in [50] it was shown that in Argentina (with yearly averaged temperatures of more than 290 K) an upgrading plant processing 250 Nm^3/h raw biogas may require 146.34 kW power and 150.25 kW cooling duty. It translates to 0.58 kWh/Nm^3 raw biogas and collectively with cooling duty to as high as 1.19 kWh/Nm^3 raw biogas. Such upgrading plants will underperform plants in colder climates where the *SPR* of less than 0.35 kWh/Nm^3 raw biogas is feasible.

8.2. Impact of plant size on power requirements

Fig. 6 quantifies the effect of increased raw biogas flow rate on specific power requirements. It is seen that by increasing plant size from 250 to 1000 Nm^3/h raw biogas processed only insignificant reduction of specific power reduction is achieved.

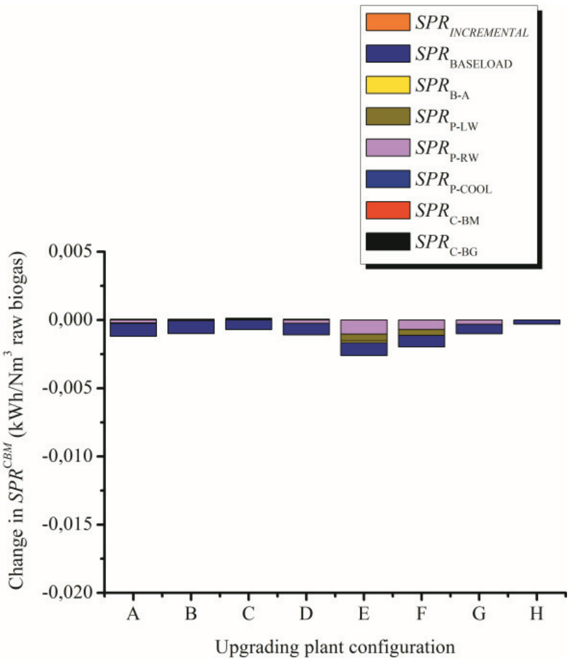

Fig. 6. Impact of increased raw biogas flow rate on the specific power requirements of various investigated biogas upgrading plants followed by biomethane compression (SPR^{CBM}). Parameters: raw biogas flow rate 1000 vs. 250 Nm^3/h, T=288.15 K.

The results of calculations shown in Fig. 6 do not however consider the impact of plant size on efficiencies of compressors and pumps which offer some additional potential for *SPR* reduction. Nevertheless, this result implies that relatively small scale biogas upgrading plants may achieve good technical performance. In other words specific power requirements are not much affected by the plant size. However, due to CAPEX reduction larger plants may have improved economics and hence overall larger plants may be to some extent more attractive for large investors. But for smaller investor distributed generation plants may be more attractive to capital constraints. In addition, smaller plants benefit from more convenient access to distributed resources such as digestible biomass for AD. Overall, in view of this result distributed generation plants may be highly productive and economic, especially when a transition from fossil resources to renewable and bioresources will finally take place.

8.3. Overview of literature data

There are very few studies reporting how power requirements are split among various upgrading and compression operations of water scrubbing. Three such studies found in literature provide data only for a HPWS plant equivalent to our configuration B (with flash followed by biomethane compression) or configuration A (only pressurised biogas upgrading). To the best of our knowledge there are no papers reporting such split data for other plant configurations, especially those investigated in our article. In addition, all these three existing publications provide numerical data which in some cases are not validated against experimental results.

More specifically, in Table 4 of [51] it is shown that the total power requirement of upgrading is 0.34 kWh/Nm^3 raw biogas which is higher than our predictions (0.21 at 0.8 MPa vs their 1 MPa) and most literature studies [2] mainly because they included cooling duty which in cold climates may be replaced by water/air cooling requiring only pumping/blowing power. In addition, for our system specific pumping power needs to be slightly higher. Their results reflect the performance of a plant processing 500 Nm^3/h raw biogas. Further, in Tables 3 and 6 of [46] the authors provide the operating results of an upgrading plant (500 Nm^3/h raw biogas, 0.8 MPa scrubbing pressure). They achieved power requirements of 0.21 kWh/Nm^3 raw biogas which is close to our predictions. Their power requirement is associated with benefits from applying an expander to recover energy of compressed biomethane (from 0.8 MPa to atmospheric pressure). This is however not possible in our case due to the fact that upgrading is followed by biomethane compression to 20 MPa. They consider relatively high power requirements for blowing air, higher than in [51] and higher than obtained in our study. Finally, in Fig. 7 of [41] the results for a smaller plant (60 Nm^3/h) are presented. It is shown that minimal power requirement is achieved at 0.8 MPa - 0.32 kWh/Nm^3 raw biogas, which is roughly the same as our predictions. They obtained higher specific pumping power requirement than in previous studies, only slightly lower than that calculate by us. In general we find their result consistent with their smaller scale plant.

9. Minimum thermodynamic work and efficiency

The minimum thermodynamic work and efficiency can be obtained from thermodynamic considerations and comparison of idealised and actual power requirements. Below we calculate minimum thermodynamic work and efficiency for biogas upgrading and biomethane compression.

9.1. Biogas upgrading

The minimum work required for biogas separation under idealised operating conditions is calculated from the combined first and second law of thermodynamics. It uses the flow rates and compositions of inlet and outlet streams and operating temperature. Fig. 7 shows a biogas upgrading plant along with an AD plant and corresponding gas streams. Stream A represents raw biogas comprising a mixture of CH_4 and CO_2 while stream B is rich in CH_4 and stream C is a mixture of CO_2 and air. Stream D is stripping air.

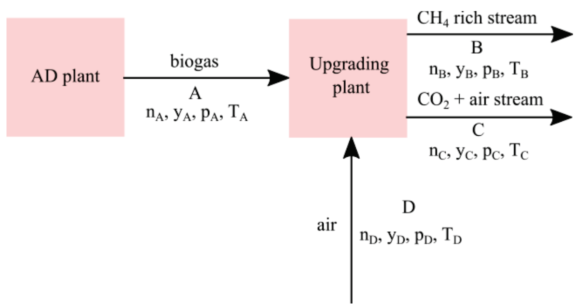

Fig. 7. Schematic of the biogas upgrading plant

The minimum work required for separating biogas mixture with the use of stripping air for an isothermal and isobaric process is equal to the negative of the difference in Gibbs free energy of the separated final states (streams B and C in Fig. 7) from the initial states (streams A and D in Fig. 7). This is the negative of Gibbs free energy of mixing. For an ideal gas the Gibbs free energy change between streams A and D to streams B and C is:

$$\mathrm{W}_{min} = \Delta G_{sep} = \Delta G_B + \Delta G_C - \Delta G_A - \Delta G_D \tag{30}$$

For an ideal mixture, the partial molar Gibbs free energy for each gas is [52-53]:

$$\frac{\partial \mathrm{G}}{\partial n_i} = G_i^0 + RT ln\left(\frac{p_i}{p}\right) \tag{31}$$

Therefore, the total Gibbs free energy of an ideal gas mixture is:

$$\mathrm{G}_{TOTAL} = \sum_i n_i \frac{\partial G}{\partial n_i} \tag{32}$$

The minimum work required to shift from states A and D to states B and C is associated with the free energy difference between the inlet and outlet streams, which can be calculated by inserting Eqs. (31) to (32) resulting in:

$$\mathrm{G}_A = n_A^{CO_2} G_{CO_2}^0 + n_A^{CH_4} G_{CH_4}^0 + RT\left(n_A^{CO_2} ln\left(y_A^{CO_2}\right) + n_A^{CH_4} ln\left(y_A^{CH_4}\right)\right) \tag{33A}$$

$$G_B = n_B^{CO_2} G_{CO_2}^0 + n_B^{CH_4} G_{CH_4}^0 + RT\left(n_B^{CO_2} ln\left(y_B^{CO_2}\right) + n_B^{CH_4} ln\left(y_B^{CH_4}\right)\right) \tag{33B}$$

$$G_C = n_C^{CO_2} G_{CO_2}^0 + n_C^{C-CO_2} G_{C-CO_2}^0 + RT\left(n_C^{CO_2} ln\left(y_C^{CO_2}\right) + n_C^{C-CO_2} ln\left(y_C^{C-CO_2}\right)\right) \tag{33C}$$

$$G_D = n_D^{CO_2} G_{CO_2}^0 + n_D^{D-CO_2} G_{D-CO_2}^0 + RT\left(n_D^{CO_2} ln\left(y_D^{CO_2}\right) + n_D^{D-CO_2} ln\left(y_D^{D-CO_2}\right)\right) \tag{33D}$$

This ideal mixing takes place at constant temperature and pressure. By substituting Eqs. (33A-D) to Eq. (30) the minimum work of separation is obtained:

$$W_{min} = RT\begin{bmatrix} n_B\left(y_B^{CO_2} ln\left(y_B^{CO_2}\right) + y_B^{CH_4} ln\left(y_B^{CH_4}\right)\right) \\ n_C\left(y_C^{CO_2} ln\left(y_C^{CO_2}\right) + \left(1 - y_C^{CO_2}\right) ln\left(1 - y_C^{CO_2}\right)\right) \\ -n_A\left(y_A^{CO_2} ln\left(y_A^{CO_2}\right) + y_A^{CH_4} ln\left(y_A^{CH_4}\right)\right) \\ -n_D\left(y_D^{CO_2} ln\left(y_D^{CO_2}\right) + \left(1 - y_D^{CO_2}\right) ln\left(1 - y_D^{CO_2}\right)\right) \end{bmatrix} \tag{34}$$

Assuming T_{SCR}= 293.15 K, $y_A^{CO_2}$= 0.35, $y_D^{CO_2}$= 0.0004, n_A/n_D = 1, specific W_{min} is calculated from Eq. (34) as 0.0046 kWh/Nm^3 raw biogas.

Since the minimum work of separation is only about 0.0046 kWh/Nm^3 it means that the upgrading process efficiency according to the second law of thermodynamics is very low, i.e. approximately 2.2% for configuration B and about 9.8% for configuration G, which suggests that there is a lot of space for improvement. The process needs to be made more reversible and reduce parasitic energy losses.

9.2. Biomethane compression

A minimum power requirement is achieved when the compression process is reversible and isothermal. In this case, the power required can be calculated from the following expression:

$$W_{min}=p_{std}q_G \ln\left(\frac{p_{out}}{p_{in}}\right) = \frac{m_G RT}{M} \ln\left(\frac{p_{out}}{p_{in}}\right) \quad (35)$$

Assuming biomethane compression from 0.8 to 20 MPa and the biomethane volumetric flow rate of 167 Nm^3/h, the minimum specific compression work calculated from Eq. (35) is 0.061 kWh/Nm^3 raw biogas. The actual work of compression under the same conditions and involving 4 compression stages with intercooling calculated in this study is about 0.11 kWh/Nm^3 raw biogas. Therefore, the compression efficiency is about 55% and there is less potential for improvement as compared to biogas upgrading discussed previously.

10. Potential of a rotary hydraulic pumping device for decreasing power requirements

Since upgrading process thermodynamic efficiency is relatively low and the lowest for configuration B (only 2.2%) there must be remarkable potential for improvement. In configuration B, which is the most widely used in European biogas upgrading plants, considerable power is consumed by water pumping between the low pressure stripper and pressurised scrubber. Therefore, by recovering energy from pressurised CO_2 loaded water and transferring it lower pressure regenerated water one can reduce associated pumping power requirements. For this purpose an energy recovery device can be used. Below we analyse the performance of a rotary hydraulic pumping device (RHPD) capable of reducing pumping power.

The rotary hydraulic pumping device integrates circulating water compression and decompression. It couples high pressure pump and decompression in one unit. It recovers decompressions energy and employs it for solvent compression [54]. It is based on a turbocharger and claimed benefits include lifetime reliability, little maintenance, scalability and flexibility to adapt to any upgrading plant conditions. The RHPD includes a multi-channel cylindrical rotor with inlet and outlet fluid passageways [55]. Pressurised water is sent to the rotor channels from where it exits in an axial direction parallel to the rotor axis. Water flow drives rotor revolution and creates a torque.

Fig. 8 explains how the RHPD can be used in an upgrading plant configuration B.

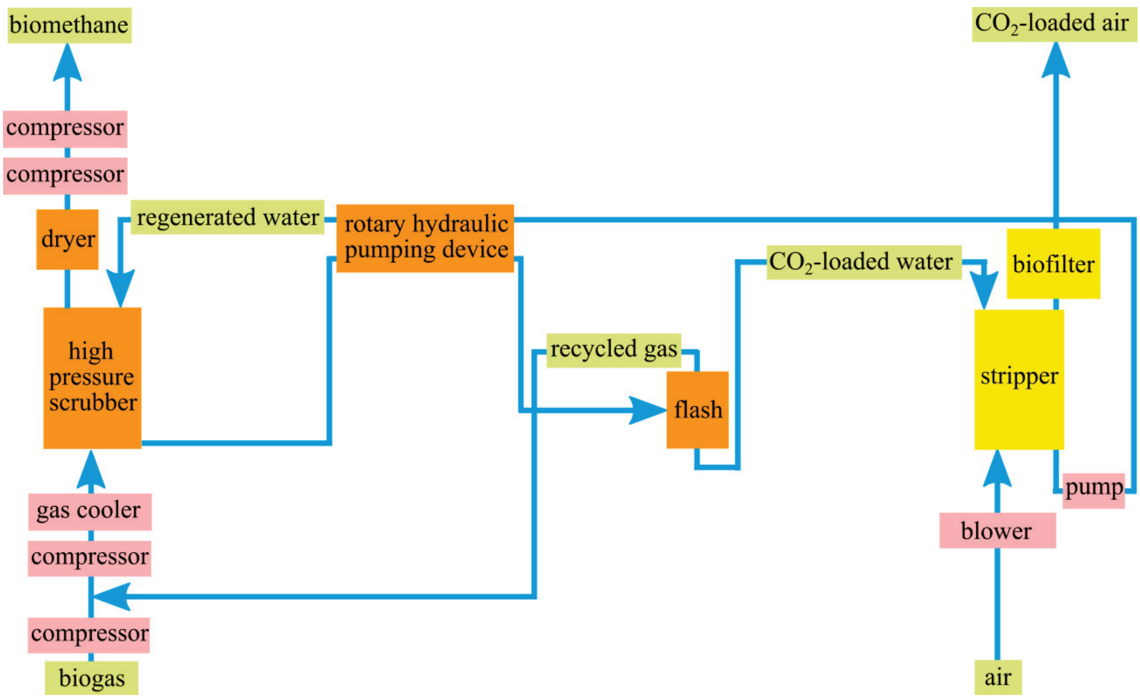

Fig. 8. Schematic of the use of the rotary hydraulic pumping device (RHPD) in the upgrading plant configuration B

The flash tank operating at 0.2 MPa is sufficient to drive water to most typical strippers. From Bernoulli equation assuming ideal flow, p_{FLS} = 0.2 MPa, p_{STR} = 0.12 MPa, w = 2.5 m/s, ρ = 999 kg/m^3 H_{STR} of 8.2 m is obtained. For the flash tank operating at 0.25 MPa H_{STR} amounts to 13 m which is compatible with the current upgrading process taking place in the plant configuration B.

$$\mathcal{H}_{\mathrm{STR}} = \frac{(p_{FLS} - p_{STR}) - \frac{w^2\rho}{2}}{\rho g} \quad (36)$$

To assess the impact of the RHPD on the upgrading plant performance we adopt its energy transfer efficiency reported in [49], η_{RHPD} = 70%. The inlet pressure of regenerated water can be calculated assuming $p_{RW,out}$ = 0.8 MPa, $p_{CLW,in}$ = 0.8 MPa, $p_{CLW,out}$ = 0.25 MPa, $q_{CLW} = q_{RW}$:

$$p_{RW,in} = p_{RW,out} - \eta_{RHPD}\left(p_{CLW,in} - p_{CLW,out}\right)\frac{q_{CLW}}{q_{RW}} \quad (37)$$

The obtained inlet pressure of regenerated water is $p_{RW,in}$ = 0.42 MPa. This pressure is used to calculate power requirements of the upgrading plant in configuration B employing the RHPD. The specific power requirement of the upgrading plant in configuration B processing 250 Nm^3 biogas at 288.15 K involving this energy recovery device is reduced by about 0.036 kWh/Nm^3 raw biogas.

11. Discussions

The differences between analysed plants configurations are mainly in upgrading while compression is not much different. The lowest specific power requirement for biogas upgrading (excluding compression) is obtained for NAPWS plants without water regeneration (0.05 kWh/Nm^3 raw biogas) but this plant requires cheap water supply, e.g. outlet water from a sewage treatment plant. All HPWS plants have specific power requirements for upgrading between 0.18 and 0.21 kWh/Nm^3 raw biogas. Other NAPWS plants have specific power requirements between 0.11 and 0.14 kWh/Nm^3 raw biogas.

The differences in specific power requirements in biomethane compression to 20 MPa are less pronounced. The compression stage adds about 0.11 kWh/Nm^3 raw biogas for HPWS plants and 0.19 kWh/Nm^3 raw biogas for NAPWS plants. The lower value for HPWS is due to biogas compression prior to upgrading to 0.8 MPa.

Biogas compression without upgrading requires 0.29 kWh/Nm^3 raw biogas which is less than most plants involving upgrading and biomethane compression. However, there are very few applications for compressed biogas and the ballast CO_2 contained in compressed biogas increases the costs of energy transport and storage. Compressed biomethane has higher energy density and is more suitable for transport or gas grid injection applications compared to compressed biogas. Transportation and gas grids require removal of CO_2. CO_2 slightly reduces efficiency of gas engines (by some 1-2%) [56]. The benefits of using biogas without upgrading and optionally without compression lie in reduced capital costs. The use of biogas in situ (e.g. through CHP) is state-of-the-art technology and compressed biomethane could compete with direct biogas use in case of high demands for biomethane, e.g. from the gas grid and transport sector.

The flash tank adds to power requirements because recycled gas increases the amount of gas for compression to 8 bar. It also slightly increases power requirements associated with the scrubber (more scrubbing water is required). So in total the contribution from flash tank is about 0.02 kWh/Nm^3 raw biogas. The main benefit from using this flash is the limited methane slip from the stripper into stripping air which for tested plants without flash is about 3.8% while for plants with flash 0.2% of methane in biogas.

Power requirements for compression include biogas and biomethane compression are slightly higher than power requirements for upgrading. In biogas upgrading power is required mainly for water pumping. The compression of biomethane/biogas is required both for transport and for grid injection applications (to about 20 MPa). The compression of biomethane is less energy intensive than the compression of raw biogas by about 0.06 kWh/Nm^3. The reason is that with biomethane there is no need to compress ballast CO_2.

Scrubbing requires lower operating temperatures and hence the performance of upgrading plants is superior in moderate and cold climates.

The power requirement of biomethane compression is relatively high (about 0.11 kWh/Nm^3 raw biogas). This power input however, enable biomethane transportation through the grid to end users. Therefore this power input in the biogas plant contributes to the transport and therefore supports the demand side making the entire business more realistic.

Specific power requirement for biomethane production is about 0.32 kWh/Nm^3 raw biogas. Since the energy content of raw biogas is about 6.0 kWh/Nm^3 it stands for 5.3%. However, assuming that electricity is obtained via CHP from biogas with efficiency 35%, 6.0 kWh$_f$/Nm^3 translates to 2.1 kWh$_{el}$/Nm^3 and hence the power consumption actually is 15.2% of the power generation potential of raw biogas. One may use biogas directly with no power requirement e.g. for CHP, heating or cooking but in this case it is unsuitable for grid injection or for transport applications. Compressed raw biogas may be used for cooking applications via bottling.

The conclusion is that wherever possible one should utilise raw biogas since it does not need upgrading or compression with associated energy penalty of about 5.3% or 15.2% (if electricity is obtained in-situ via biogas CHP). However, if biogas needs to be used remotely (transportation or gas grids) it needs to be upgraded and compressed.

The investigated impacts of temperature revealed interesting plant performance. The minimum works of upgrading and compression are roughly proportional to temperature. However, with drop in T by 1.7% the actual reduction of power requirement was more pronounced, between 4 and 5%. This is explained by highly non-linear nature of CO_2 solubility in water. The reduction in compression power requirement was smaller than the reduction in upgrading *SPR* (see Fig. 6) and roughly proportional to temperature change which is explained by more linear compression process nature. This again emphasises that water scrubbing is a more suitable technology for moderate and colder climates which is not the case for other upgrading technologies such as membranes which do not have similar temperature dependence.

The impacts of plant size are less pronounced. Taking into account that smaller plants benefit from more convenient access to distributed resources such as digestible biomass for AD the study suggests that such small plants may be highly productive and economic.

There is potential to recover some of the power required to operate the upgrading plant. For example, by applying the rotary hydraulic pumping device in the state-of-the-art upgrading plant in configuration B the power requirement for pumping water to the pressurised scrubber can be reduced by about 0.036 kWh/Nm^3 raw biogas. This turbocharger transfers energy from the high pressure CO_2 loaded water to the low pressure regenerated water with efficiency of about 70% [49].

12. Conclusions

This study applies the same methodology for evaluation of various biomethanation plants. Specific power requirements of eight biogas upgrading and compression plants configurations are calculated. The results show that reduced power requirement is feasible in plants without water regeneration and without flash. For optimised plants including water regeneration and flash the power requirement is about 0.32 kWh/Nm^3 raw biogas.

For plants with specific power requirement of 0.32 kWh$_{el}$/Nm^3 raw biogas and the energy content of raw biogas of 6 kWh$_f$/Nm^3 (equivalent of 2.1 kWh$_{el}$/Nm^3) biogas is converted to biomethane with power consumption of less than 15.2% (or with efficiency

84.8%). However, from the calculated minimum works of upgrading (0.0046 kWh/Nm^3 raw biogas) and of biomethane compression (0.061 kWh/Nm^3 raw biogas) the obtained overall plant thermodynamic efficiency is much lower, i.e. about 20.5%. Especially biogas upgrading is inefficient compared to its thermodynamic limits with typical thermodynamic efficiencies between 2.2 and 9.8% depending on plant configuration while biogas compression has higher thermodynamic efficiency of about 55%. It emphasises that biogas upgrading may have remarkable potential for power requirement reduction.

The study evaluates the potential for minimising energy dissipation in the state-of-the-art HPWS upgrading plant with flash (configuration B) by applying the rotary hydraulic pumping device at about 0.036 kWh/Nm^3 raw biogas. It increases the thermodynamic efficiency of upgrading from about 2.2% to about 2.7% (by 23%) proving that remarkable progress in improving energy efficiency is realistic.

From comparison of HPWS (with flash) and NAPWS (with water regeneration) plants, it is found that although they have similar specific power requirements. They differ in methane slip being more significant for NAPWS. Reduced operating temperatures have lower power requirements meaning that the water scrubbing is more suitable for moderate and colder climates. The plant size has small impact on specific power requirements meaning that distributed generation plants may be highly productive and economic, especially when a transition from fossil resources to renewable and bioresources will finally take place.

The results of this study have implications for sustainability of biomethane because they provide insights into how parasitic power requirements are structured and how they can be controlled.

Nomenclature

$\mathcal{A}$	interfacial area density of a column, 1/m
CAPEX	capital expenditure
CHP	combined heat and power
C_p	specific heat, J/(kg K)
$\mathcal{D}$	column or pipe diameter, m
d	pipeline diameter, m
f	Colebrook-White friction coefficient, -
G	Gibbs free energy, J
g	acceleration of gravity, m/s^2
H	liquid head, m
$\mathcal{H}$	column height, m
H_i	Henry constant of species i, $(Pa\ m^3)/mol$
HPWS	high pressure water scrubbing
K_L	global gas-liquid mass transfer coefficient, m/s
L	pipeline length, m
M	molar mass, kg/mol
m	mass flow rate, kg/s
n	number of compression stages, -
N	mass transfer flux, mol/s
NAPWS	near-atmospheric water scrubbing
OPEX	operating expenditure
p	pressure, Pa
p^{std}	standard pressure = $1.013\ 10^5$Pa
PR	power requirement, W
Δp	pressure drop of fluid, Pa

RHPD	rotary hydraulic pumping device
q	volumetric flow rate, m^3/s or Nm^3/s or Nm^3/h
	1 Nm^3 = 1 m^3 at 1.013 10^5Pa, 273.15K
Q	mass flow rate, kg/s
R	universal gas constant = 8.314 J/(K mol)
Re_L	Reynolds number (ρLuLdH)/μL or (ρLuL)/(awμL)
S	free interface area, m^2
SPR	specific power requirement, W/Nm^3
t	time, s
T	temperature, K
u	superficial velocity, m/s
VLE	vapour-liquid equilibrium
W	work, J; specific work, J/Nm^3
x	mass fraction, kg/kg
y	molar fraction, mol/mol
z	column height coordinate, m
ε	pipe surface roughness, -
εp	packing void fraction, m^3/m^3
η	efficiency, -
κ	ratio of specific heats = 1.32 (CH_4), 1.28 (CO_2)
μ	dynamic viscosity, kg/(m s)
v	kinematic viscosity, m^2/s
ξ	performance index, -
ρ	fluid density, kg/m^3
σ	surface tension, N/m

σ_C	critical surface tension of packing material, N/m
τ	gas-liquid mass transfer rate density, kg/(m s)
Φ	enhancement factor for turbulent diffusion
ϕp	form factor, -
Ω	column cross-section area, m^2
[ ]	molar concentration of a species, mol/m^3

Subscripts and superscripts

ATM	atmospheric
C	compressor
CG	gas phase constant
CL	liquid phase constant
CLW	CO_2 loaded water
COOL	coolant
CPK	packing specific constant
D	dynamic
e	enriched biogas
FLS	flash tank
G	gas phase
in	inlet
L	liquid phase
out	outlet
r	raw biogas
RW	regenerated water
S	static

SCR scrubber

std at standard p=1.013 10^5Pa and T=298.15K

STR stripper

TK degassing tank

T total

w water

Acknowledgements

This study has been supported by the members of the Renewable Energy and Sustainable Development (RESD) Group (Poland) which is gratefully acknowledged.

References

[1] Thrän D, Billig E, Persson T, Svensson M, Daniel-Gromke J, Ponitka J, Seiffert M, Baldwin J, Kranzl L, Schipfer F, Matzenberger J, Devriendt N, Dumont M, Dahl J, Bochmann G. Biomethane - status and factors affecting market development and trade. eds. Junginger M, Baxter D. IEA Task 40 and Task 37 Joint Study, 2014.

[2] Sun Q, Li H, Yan J, Liu L, Yu Z, Yu X. Selection of appropriate biogas upgrading technology - a review of biogas cleaning, upgrading and utilisation. Renewable and Sustainable Energy Reviews 2015;51:521-532.

[3] Abatzoglou N, Boivin S. A review of biogas purification processes. Biofuels Bioprod Biorefin 2009;3:42-71.

[4] Ryckebosch E, Drouillon M, Vervaeren H. Techniques for transformation of biogas to biomethane. Biomass Bioenergy 2011;35:1633-45.

[5] Budzianowski WM. Benefits of biogas upgrading to biomethane by high-pressure reactive solvent scrubbing. Biofuels Bioprod Biorefin 2012;6(1):12-20.

[6] Beil M, Beyrich W. Biogas upgrading to biomethane. The Biogas Handbook. eds Wellinger A, Murphy J, Baxter D. Woodhead Publishing. 2013:342-377.

[7] IEA (International Energy Agency). Country report Germany. IEA Bioenergy Task 37. Angers. 2014.

[8] Malmberg Water AB. Upgrade biogas to biomethane with reliable technology. Åhus: Malmber Water AB. 2014.

[9] Budzianowski WM, Budzianowska DA. Economic analysis of biomethane and bioelectricity generation from biogas using different support schemes and plant configurations. Energy 2015;88:658-66.

[10] Bortoluzzi G, Gatti M, Sogni A, Consonni S. Biomethane production from agricultural resources in the Italian scenario: techno-economic analysis of water wash. Chem Eng Trans 2014;37:259-64.

[11] Häkansson A. Preventing microbial growth on pall-rings when upgrading biogas using absorption with water wash. Svenskt Gastekniskt Center. Report 166. 2006.

[12] Zhou X, Yuan S, Wu C, Song B, Peng S. Potential production and distribution of microalgae in China. J Renew Sustain Energy 2013;5:art. no. 053101.

[13] Ertit Taştan B, Duygu E, Ilbaş M, Dönmez G. Utilization of LPG and gasoline engine exhaust emissions by microalgae. Journal of Hazardous Materials 2013;246-247:173-80.

[14] Muradov N, Taha M, Miranda AF, Kadali K, Gujar A, Rochfort S, Stevenson T, Ball AS, Mouradov A. Dual application of duckweed and azolla plants for wastewater treatment and renewable fuels and petrochemicals production. Biotechnol Biofuels 2014;7:30.

[15] Xu JL, Shen GX. Growing duckweed in swine wastewater for nutrient recovery and biomass production. Bioresour Technol 2011;102:848-53.

[16] Budzianowski WM. Tetra-stable bifurcation structure of the climate system of Earth: Mechanisms triggering potential transition to the greenhouse steady state. Int J Glob Warm 2013;5(2):152-78.

[17] Tamhankar Y, King B, Whiteley R, Resetarits M, Cai T, Aichele C. Aqueous amine spray absorption and droplet distribution data for CO_2 capture applications. Energy Procedia 2014;63:293-300.

[18] Whitman W. The two-film theory of absorption. Chem Metal Eng 1923;29:146.

[19] Trambouze P, Euzen JP. Chemical reactors: from design to operation. Paris: Editions Technip; 2004.

[20] Coulson J, Richardson J. Chemical Engineering Vol. 1: Fluid Flow, Heat Transfer and Mass transfer, 6th ed. Butterworth: Heinemann; 1999.

[21] Danckwerts P.V. Gas-liquid reactions. New York: MacGraw-Hill;1970.

[22] Vas Bhat R, Kuipers J, Versteeg G. Mass transfer with complex chemical reactions in gas-liquid systems: two-step reversible reactions with unit stoichiometric and kinetic orders. Chem Eng J 2000;76:127-52.

[23] Onda K, Takeuchi H, Okumoto Y. Mass transfer coefficients between gas and liquid phases in packed columns. J Chem Eng Jpn 1968.

[24] Versteeg GF, Van Swaaij WPM. Solubility and diffusivity of acid gases (CO_2, N_2O) in aqueous alkanolamine solutions. J Chem Eng Data 1988;33:29-34.

[25] Wylock C, Dehaeck S, Cartage T, Colinet P, Haut B. Experimental study of gas-liquid mass transfer coupled with chemical reactions by digital holographic interferometry. Chem Eng Sci 2011;66:3400-12.

[26] Sander R. Compilation of Henry's Law constants for inorganic and organic species of potential importance in environmental chemistry. http://www.mpch-mainz.mpg.d/~sander/res/henry.html. 1999.

[27] Broecker WS, Peng TH. Gas exchange rates between air and sea. Tellus 1974;26:21-35.

[28] Huttunen JT, Väisänen TS, Hellsten SK, Martikainen PJ. Methane fluxes at the sediment-water interface in some boreal lakes and reservoirs. Boreal Environ Res 2006;11:27-34.

[29] Guo H, Chen Y, Lu W, Li L, Wang M. In situ Raman spectroscopic study of diffusion coefficients of methane in liquid water under high pressure and wide temperatures. Fluid Phase Equilibria 2013;360:274-8.

[30] Reid RC, Prausnitz JM, Poling BE. The properties of gases and liquids. New York: McGraw-Hill; 1986.

[31] Wylock C, Antuñano N, Arias PL, Haut B. Analysis of the simultaneous gas-liquid CO_2 absorption and liquid-gas NH_3 desorption in a hydrometallurgical Waelz oxides purification process. Int J Chem Reactor Eng 2014;12:1-14.

[32] Cowie, Watt. Diffusion of methane and chloromethanes in air. Canadian Journal of Chemistry 1971;49:74.

[33] Edwards TJ, Maurer G, Newman J, Prausnitz JM. Vapor-liquid equilibria in multicomponent aqueous solutions of volatile weak electrolytes. AIChE J 1978;24:966-76.

[34] Hikita H, Asai S, Takatsuka T. Absorption of carbon dioxide into aqueous sodium hydroxide and sodium bicarbonate solutions. Chem Eng J 1976;11:131-41.

[35] Cents AHG, Brilman DWF, Versteeg GF. CO_2 absorption in carbonate/bicarbonate solutions: the Danckwerts-criterion revisited. Chem Eng Sci 2005;60:5830-5.

[36] Tsonopoulos C. Ionization constants of water pollutants. J Chem Eng Data 1976;21:190-3.

[37] Wylock CE, Budzianowski WM, Marciniak PA. Modelling and simulation analysis of water scrubbing of biogas. abstract submitted to GLS-13 conference for possible publication in Chemical Engineering Science.

[38] Cussler EL. Diffusion: mass transfer in fluid systems. Ch. 8: fundamentals of mass transfer. 3rd edition, Cambridge: Cambridge University Press; 2009.

[39] Cozma P, Wukovits W, Mămăligă I, Friedl A, Gavrilescu M. Modeling and simulation of high pressure water scrubbing technology applied for biogas upgrading. Clean Technol Environ Policy 2015;17:373-91.

[40] Han IS, Han C. Modeling of multistage air-compression systems in chemical processes. Ind Eng Chem Res 2003;42:2209-18.

[41] Nock WJ, Walker M, Kapoor R, Heaven S. Modeling the water scrubbing process and energy requirements for CO_2 capture to upgrade biogas to biomethane. Ind Eng Chem Res 2014;53(32):12783-92.

[42] Läntelä J, Luostarinen J. D5.4 Results of design, construction and testing of low-cost modular biogas upgrading systems. Deliverable of EU FP7VALORGAS project. 2013.

[43] Chandra R, Vijay VK, Subbarao PMV. Vehicular quality biomethane production from biogas by using an automated water scrubbing system. ISRN Renewable Energy 2012;2012:904167.

[44] Huang L, Qing C, Tao H, Wang Y, Liu X. Experimental study for biogas upgrading by water scrubbing under low pressure. The Open Chemical Engineering Journal 2015;9:34-38.

[45] Götz M, Köppel W, Reimert R, Graf F. Optimierungspotenzial von Wäschen zur Biogasaufbereitung. Teil 1-Physikalische Wäschen. Chemie Ingenieur Technik 2011;83(6):858-866.

[46] Xu Y, Huang Y, Wu B, Zhang X, Zhang S. Biogas upgrading technologies: energetic analysis and environmental impact assessment. Chinese Journal of Chemical Engineering 2015;23(1):247-54.

[47] Avci A, Karagoz I. A novel explicit equation for friction factor in smooth and rough pipes. ASME J Fluids Eng 2009;131:061203.

[48] http://encyclopedia.airliquide.com. accessed 2015-11.

[49] Krish P, Gains-Germain A, Thorp J, Martin J, Shirazi M. Optimizing amine process design using liquid phase turbochargers. Proceedings of ASME Turbo Expo 2015: Turbine Technical Conference and Exposition GT2015. Montréal. Canada. June 15-19. 2015.

[50] Morero B, Groppelli E, Campanella EA. Life cycle assessment of biomethane use in Argentina. Bioresource Technology 2015;182:208-216.

[51] Cozma P, Ghinea C, Mămăligă I, Wukovits W, Friedl A, Gavrilescu M. Environmental impact assessment of high pressure water scrubbing biogas upgrading technology. Clean Soil Air Water 2013;41:917-927.

[52] Gaskell D. Introduction to the thermodynamics of materials. Taylor & Francis. Washington D.C. 1995.

[53] House KZ, Harvey CF,Aziz MJ, Schrag DP. The energy penalty of post-combustion CO_2 capture & storage and its implications for retrofitting the U.S. installed base. Energy Environ Sci 2009;2:193-205.

[54] Energy Recovery Inc. IsoBoost. www.energyrecovery.com. accessed 2016-01.

[55] Pinto JM, Martin JG, Stover RL. Rotary energy recovery device. Patent no. WO 2011/079045 A2. 2011.

[56] Jenbacher. Jenbacher type 4. The new 4B version - an efficiency milestone. GE Jenbacher GmbH, Jenbach, Austria, 2015.